INFORME **DFN/IN-03/II-22**

REF. EXTERNA

REPORT ON S/U ANALYSES IN MYRRHA HOMOGENIZED MODEL V1.8 PERFORMED WITH THE MCNP 6.2 AND SUMMON CODES AND THE JEFF-3.3 LIBRARY

DIVISIÓN DE FISIÓN NUCLEAR

Ciemat Centro de Investigaciones Energéticas, Medioambientales y Tecnológicas

TITULO: Report on S/U analyses in MYRRHA homogenized model v1.8 performed with the MCNP6.2 and SUMMON codes and the JEFF-3.3 library

AUTORES: S. Panizo, V. Bécares

ABSTRACT:

This report presents nuclear data sensitivity and uncertainty (S/U) analyses for several safety-related reactor parameters (k_{eff}, β_{eff} and reactivity coefficients) of the latest design (version 1.8) of the MYRRHA facility. This work has been performed within the frame of task 5.1 of EU H2020 SANDA project using the codes MCNP 6.2 and SUMMON, the JEFF-3.3 nuclear data library and an homogenized model of MYRRHA version 1.8 supplied by SCK CEN. In this report, nominal values for these parameters, integrated sensitivity coefficients (ISCs), sensitivity profiles for the major nuclear reactions with the highest contributions to the uncertainty, the total uncertainty due to nuclear data and top reactions contributing to the uncertainty are provided. As a conclusion, and although major contributors to the uncertainty depend on the specific parameter, in general, the major reaction contributors are elastic and inelastic reactions in fuel, coolant and structural materials. Nevertheless, given the slow convergence of sensitivity calculations with these reactions, more detailed simulations will be required to fully understand these contributions.

	NOMBRE	FIRMA	FECHA	
Preparado por:	S. Panizo			
Revisado por:	F. Álvarez			
Conf por A. C.:	S. Fernández			FECHA DE EMISIÓN
Aprobado por:	E. González			

CONTENTS

1. INTRODUCTION

EC H2020 SANDA project (*Supplying Accurate Nuclear Data for energy and non-energy Applications*) aims to enhance the quality of nuclear data by coordinating European activities in the whole nuclear data cycle, ranging from new measurements in both differential and integral experiments to evaluation, validation and dissemination activities.

In Task 5.1 the focus is on quantifying the impact of nuclear data uncertainties on the design and safety parameters of advanced reactors and determining the sources of these uncertainties. Besides, the work performed within this task will help to improve the JEFF-3.3 nuclear data library and other future releases such as JEFF-4.0. These developments will be relevant in the operation, design and licensing processes. Among the advanced nuclear reactor designs chosen for sensitivity and uncertainty (S/U) analyses within SANDA Task 5.1 is included MYRRHA (*Multi-purpose HYbrid Research Reactor for High-tech Applications*) [SCK CEN 2021], an up to 100 MWth, LBE-cooled fast reactor with both critical and subcritical modes of operation (in the second case, coupled to an accelerator-driven spallation source). The MYRRHA project is currently in the pre-licensing phase that demands safety estimations for the core design. In this report, the contribution to the assessment is focused on the impact of nuclear data in the uncertainties.

S/U analysis for MYRRHA design version 1.6 [Malambu 2014] was already performed within the EC FP7 CHANDA (*solving CHAllenges in Nuclear Data*) project. Parameters analysed include k_{eff} [Romojaro 2015], β_{eff} [Kodeli 2015] and reactivity coefficients [Romojaro 2019]. However, an update is necessary since the MYRRHA core design has evolved and new nuclear data libraries have been released in the meantime. In this work, S/U analyses are performed in a simplified, homogenized model of MYRRHA core version 1.8 [Fiorito 2021a].

The changes in version 1.8 with respect to the previous version (v1.6) are a reduction in the core size and a new choice of the reflector material, replacing beryllium with MgO [Fiorito 2019]. In the homogenized model used in this work, the reactor and core components were homogenized radially in each assembly and vertically in several regions. Therefore, the materials were also homogenized. All the components located outside the core barrel were neglected in this model. The fuel assembly homogenized model consists of five axial regions: a 65cm-long fuel column, two 3.5cm-long cylindrical reflectors located up and down the fuel column and then two homogenized parts that contain everything that is above the upper reflector and everything that is below the lower reflector.

In order to support the licensing of MYRRHA, SCK CEN has requested S/U analysis for several reactor parameters [Fiorito 2021b], namely:
- The criticality constant (k_{eff}) (Section 3.1)
- The effective delayed neutron fraction (β_{eff}) (Section 3.2)
- The Doppler coefficient at different temperatures (Section 3.5)
- The void coefficient for different void scenarios (Section 3.3)
- The reactivity worth value for the case of a control rod insertion (Section 3.4)
- The power peaking factor.

For each of these parameters, it is requested (1) its nominal value; (2) the sensitivity profiles and Integrated Sensitivity Coefficients (ISC) of the top 10 contributors; and the total uncertainty and top 10 contributors to the uncertainty due to nuclear data.

This work describes the S/U analyses carried out at CIEMAT for the first five of these points. They have been performed with the SUMMON code for the MYRRHA 1.8 homogenized model in combination with sensitivity profiles calculated with MCNP 6.2 [Werner 2017] and the JEFF-3.3 library [Plompen 2020]. Performing S/U analyses for the power peaking factor is more complex (see Section 2) and will be presented in another report.

2. SUMMON

The propagation of the uncertainty in the nuclear data to nuclear reactor parameters is a complex problem that requires considerable computational effort. This complexity mainly is due to the correlations existing between different energy groups of a given reaction cross section, as well as between the cross sections of different nuclear reactions. These correlations are quantified in the covariance matrices that are included in the latest releases of the nuclear data libraries. With these covariance matrices, together with the sensitivity profiles of the reactor parameters to the nuclear data, the uncertainty due to the nuclear data can be propagated to the reactor parameters using the *sandwich rule*:

$$\sigma_R^2 = s_{R,\alpha} C_{\alpha\alpha} s_{R,\alpha}^T \quad (2.1)$$

where the variance of a certain parameter, σ_R^2, is calculated from the covariance matrix, $C_{\alpha\alpha}$, and the sensitivity profile of the parameter R to the set of nuclear data $\alpha = (\alpha_1, \ldots, \alpha_N)$ $S_{R,\alpha}$ defined as:

$$s_{R,\alpha} = \left(\frac{\alpha_1}{R}\frac{\partial R}{\partial \alpha_1}, \ldots, \frac{\alpha_k}{R}\frac{\partial R}{\partial \alpha_k}\right) \quad (2.2)$$

Usually, α refers to a nuclear reaction cross section divided into N energy groups collapsed to a particular energy group for the nuclear data $\alpha = (\alpha_1, \ldots, \alpha_N)$.

To perform this error propagation, the SUMMON (*Sensitivity and Uncertainty Methodology for Monte Carlo codes*) [Romojaro 2017] has been developed at CIEMAT. SUMMON performs sensitivity and uncertainty calculations for critical reactor parameters using covariance matrices included in state-of-the-art nuclear data libraries and sensitivity profiles in the *Sensitivity Data File* (SDF) format ([Rearden 2018], section 6.3.A) calculated with Monte Carlo codes. In this report, the covariance matrices from JEFF-3.3 have been used, processed in 33 energy groups [Palmiotti 2010] with NJOY [NJOY 21], alongside sensitivity profiles calculated with the MCNP 6.2 KSEN card. This card provides sensitivity profiles only for the k_{eff}, but from them SUMMON calculates sensitivity profiles for other derived reactor parameters (β_{eff}, reactivity coefficients). However, for the case of power peaking factors, sensitivity profiles of fission rates are required, instead of sensitivity profiles of k_{eff}. While these coefficients can be in principle calculated with the PERT card of MCNP, dealing with these coefficients has to be implemented in SUMMON and a detailed assessment of the quality and usefulness of the results has to be performed. For this reason, S/U analyses for the power peaking factors have not been included in this work.

Another point that has to be taken into account is that the variance σ_R^2 only takes into account the variance due to the uncertainty in the nuclear data, expressed in the covariance matrix. However, when the sensitivity profiles are calculated with a Monte Carlo code, they are also affected by statistical errors. Hence, it is necessary to calculate as well the statistical error in σ_R^2. In SUMMON it has been recently implemented this calculation of the total statistical error. It has also been compared with the result of several Monte Carlo simulations with different random number sequences. However, this last scheme is very time-consuming and has only been applied to some of the parameters analyzed in this work, namely the k_{eff}, the β_{eff}, one of the void scenarios and one of the control rods insertion scenarios.

3. RESULTS

3.1. THE CRITICALITY CONSTANT, k_{eff}

The value of the criticality constant obtained with the MYRRHA homogenized model is:

$$k_{eff} = 1.01542 \pm 0.00003$$

The reactions with the largest contributions to the uncertainty of the criticality constant are presented in Table 1. It also includes the total contribution to the uncertainty calculated including all reactions and not only the ones that are listed.

The first column of Table 1 presents the correlations between two reactions. When a single reaction appears twice, this means that it is correlated with itself, meaning that the correlation happens between different energy groups of the same reaction.

Table 1. Reactions with the largest contributions to the uncertainty in the criticality constant of the MYRRHA homogenized model calculated with MCNP+KSEN2sdf+SUMMON with JEFF-3.3 library.

MYRRHA - JEFF-3.3						
Quantity				k_{eff} uncertainty (%)		
^{240}Pu	(n,f)	^{240}Pu	(n,f)	5.54E-01	±	6.61E-04
^{240}Pu	(n,f)	^{240}Pu	(n,γ)	-4.32E-01	±	1.72E-04
^{239}Pu	Prompt Fission ν	^{239}Pu	Prompt Fission ν	3.15E-01	±	2.03E-04
^{239}Pu	(n,f)	^{239}Pu	(n,f)	2.77E-01	±	3.20E-04
^{239}Pu	Total Fission χ	^{239}Pu	Total Fission χ	2.37E-01	±	2.88E-03
^{240}Pu	(n,γ)	^{240}Pu	(n,γ)	2.01E-01	±	8.37E-05
^{239}Pu	(n,f)	^{239}Pu	(n,γ)	1.82E-01	±	1.13E-04
^{238}U	(n,γ)	^{238}U	(n,γ)	1.72E-01	±	6.81E-05
^{238}U	(n,n')	^{238}U	(n,f)	-1.40E-01	±	3.66E-04
^{238}U	(n,n')	^{238}U	(n,n')	1.32E-01	±	3.24E-03
^{239}Pu	(n,γ)	^{239}Pu	(n,γ)	1.27E-01	±	1.74E-04
^{238}U	(n,f)	^{238}U	(n,γ)	1.21E-01	±	7.30E-05
^{238}U	(n,f)	^{238}U	(n,f)	1.14E-01	±	2.89E-04
^{238}U	(n,n')	^{238}U	(n,γ)	9.62E-02	±	1.81E-04
^{241}Pu	Total Fission χ	^{241}Pu	Total Fission χ	8.50E-02	±	1.20E-03
^{208}Pb	(n,n)	^{208}Pb	(n,n)	8.24E-02	±	4.08E-03
^{56}Fe	(n,γ)	^{56}Fe	(n,γ)	7.71E-02	±	1.57E-04
^{241}Pu	Total Fission ν	^{241}Pu	Prompt Fission ν	7.57E-02	±	5.63E-05
^{56}Fe	(n,n)	^{56}Fe	(n,n)	7.16E-02	±	3.55E-03
^{238}Pu	Total Fission ν	^{238}Pu	Prompt Fission ν	7.13E-02	±	5.07E-05
			k_{eff} total uncertainty (%) =	7.62E-01	±	1.26E-03

The main contributions to the uncertainty of the k_{eff} are fission and capture reactions in plutonium isotopes ^{239}Pu and ^{240}Pu. They are also noticeable contributions of the inelastic reaction of ^{238}U and inelastic reactions of ^{208}Pb and ^{56}Fe. The total contribution due to nuclear data in the criticality constant is around 0.76%.

Sensitivity profiles of the major contributors to the uncertainty will be adjunct as a compressed file with this report but two examples are shown in Figures Figure 1 and Figure 2 below.

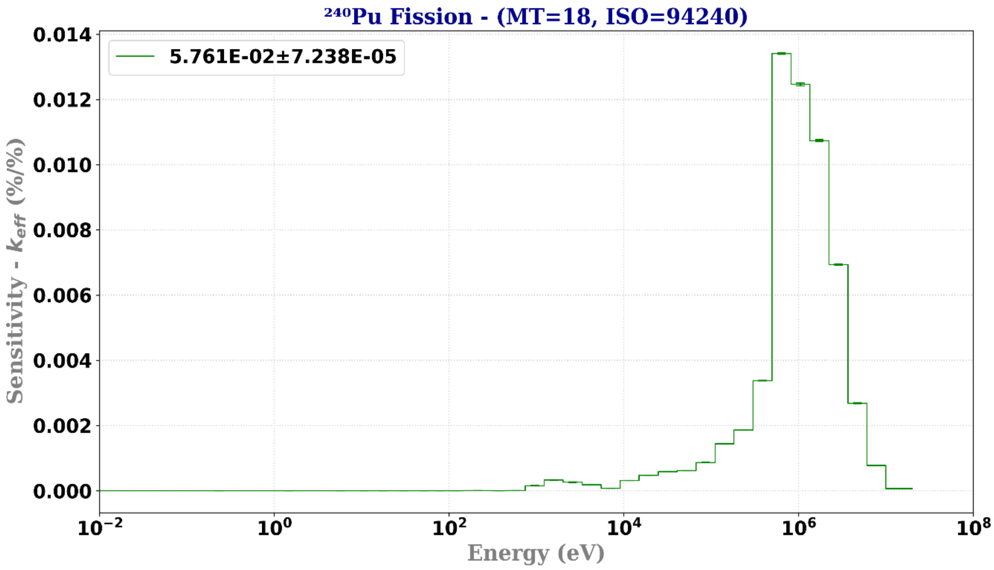

Figure 1. Sensitivity profile for the fission reaction (n,f) of ^{240}Pu.

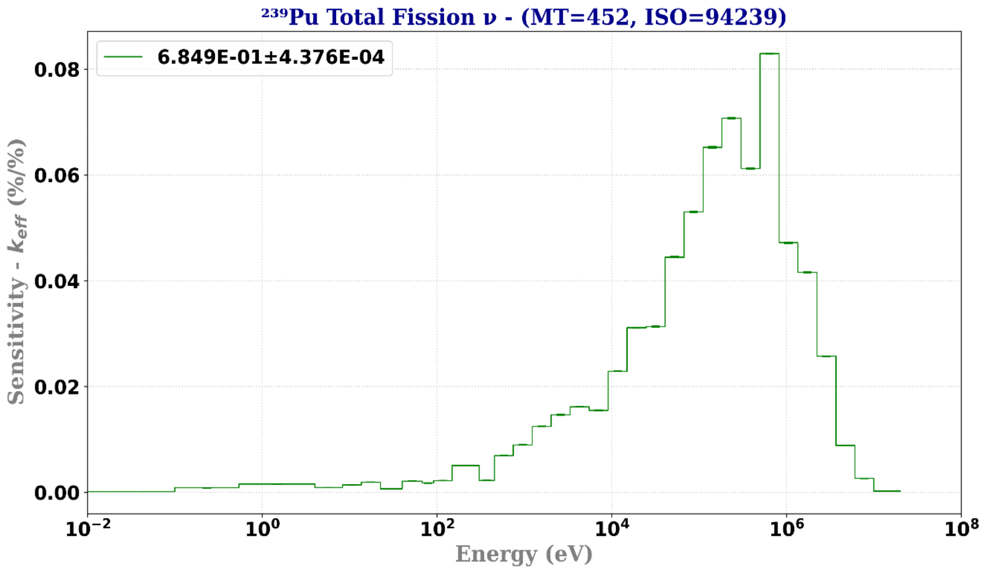

Figure 2. Sensitivity profile for the total fission ν of ^{239}Pu.

The Integrated Sensitivity Coefficients are listed in Table 2 for the major contributors (in absolute value) but also in each sensitivity profile for each pair isotope-reaction.

As described in section 2, the calculation of the statistical errors of the total uncertainty in k_{eff} can be preliminary compared with the estimation determined as the standard deviation of the results of a total of eight Monte Carlo calculations with different random number sequences. The result obtained in this way is:

$$k_{eff} \text{ total uncertainty (\%)} = 0.762 \pm 0.001$$

As can be seen, the statistical errors of the total uncertainty calculated by these two methods are essentially identical.

The statistical error of some of the reactions with the highest contribution to the uncertainty has been also calculated with this methodology:

$$[\,^{240}Pu(n,f) - \,^{240}Pu(n,f)\,] \text{ uncertainty contribution (\%)} = 0.554 \pm 3.16 \cdot 10^{-4}$$

$$[\,^{240}Pu(n,f) - \,^{240}Pu(n,\gamma)] \text{ uncertainty contribution (\%)} = -0.431 \pm 1.94 \cdot 10^{-4}$$

$$[\,^{239}Pu \text{ (Prompt Fission } \nu) - \,^{239}Pu \text{ (Prompt Fission } \nu)] \text{ uncertainty contribution (\%)} = 0.315 \pm 4.44 \cdot 10^{-5}$$

Notice that although these error estimates can differ from the statistical error values provided by SUMMON (in particular, in the third case is about 25%), the order of magnitude is comparable. Further studies are required to understand this behaviour.

Table 2. ISC for the major contributions to the k_{eff} uncertainty due to nuclear data. ISC obtained with MCNP and JEFF-3.3 library.

Quantity		ISC (%/%)		
^{239}Pu	Total Fission ν	6.849E-01	±	4.376E-04
^{239}Pu	Prompt Fission ν	6.835E-01	±	4.350E-04
^{239}Pu	Fission	4.771E-01	±	4.434E-04
^{238}U	(n,γ)	-1.085E-01	±	6.078E-05
^{241}Pu	Total Fission ν	9.891E-02	±	7.205E-05
^{241}Pu	Prompt Fission ν	9.844E-02	±	7.157E-05
^{240}Pu	Total Fission ν	8.490E-02	±	7.415E-05
^{240}Pu	Prompt Fission ν	8.467E-02	±	7.394E-05
^{238}U	Total Fission ν	7.216E-02	±	9.648E-05
^{238}U	Prompt Fission ν	7.107E-02	±	9.526E-05

3.2. THE EFFECTIVE DELAYED NEUTRON FRACTION, β_{eff}

The effective delayed neutron fraction can be defined as the ratio between the adjoint weighted delayed neutron production ($P_{d,eff}$) and the total neutron production ($P_{d,eff}$) and rewrited as follows:

$$\beta_{eff} = \frac{P_{d,eff}}{P_{eff}} = 1 - \frac{k_p}{k_{eff}} \quad (3.2.1)$$

being k_p the effective multiplication factor if only prompt neutrons are considered and k_{eff} the criticality constant. SUMMON can calculate the β_{eff} with two different methodologies: the Brestcher's approximation [Bretscher, 1997] and Chiba's method [Chiba, 2009].

3.2.1. Brestcher's method

The effective delayed neutron fraction determined using the Brestcher's approximation is:

$$\beta_{eff} = 342 \pm 4 \text{ pcm}$$

Table 3. Reactions with the largest contributions to the uncertainty in the effective delayed neutron fraction of the MYRRHA homogenized model calculated with MCNP+KSEN2sdf+SUMMON with JEFF-3.3 library using the Brestcher's approximation.

MYRRHA - JEFF-3.3						
Quantity				β_{eff} uncertainty (%)		
^{56}Fe	(n,n)	^{56}Fe	(n,n)	3.69E+00	±	1.27E+00
^{238}U	(n,n')	^{238}U	(n,n')	2.72E+00	±	1.37E+00
^{238}U	(n,n)	^{238}U	(n,n')	-2.31E+00	±	1.21E+00
^{241}Pu	(n,n)	^{241}Pu	(n,n)	2.12E+00	±	1.48E+00
^{58}Ni	(n,n)	^{58}Ni	(n,n)	1.96E+00	±	8.07E-01
^{16}O	(n,n)	^{16}O	(n,n)	1.78E+00	±	1.13E+00
^{57}Fe	(n,n)	^{57}Fe	(n,n)	1.72E+00	±	1.04E+00
^{240}Pu	(n,n)	^{240}Pu	(n,n)	1.72E+00	±	6.36E-01
^{238}U	(n,n)	^{238}U	(n,n)	1.18E+00	±	1.21E+00
^{55}Mn	(n,n)	^{55}Mn	(n,n)	1.14E+00	±	9.39E-01
^{54}Fe	(n,n)	^{54}Fe	(n,n)	1.11E+00	±	7.77E-01
^{238}U	(n,n')	^{238}U	(n,f)	1.11E+00	±	3.66E-01
^{58}Fe	(n,n)	^{58}Fe	(n,n)	1.10E+00	±	3.72E-01
^{208}Pb	(n,n)	^{208}Pb	(n,n)	1.01E+00	±	1.48E+00
^{238}U	(n,n)	^{238}U	(n,f)	-9.55E-01	±	2.92E-01
^{239}Pu	Total Fission χ	^{239}Pu	Total Fission χ	9.54E-01	±	1.17E+00
^{238}U	(n,n')	^{238}U	(n,γ)	-8.39E-01	±	2.31E-01
^{62}Ni	(n,n)	^{62}Ni	(n,n)	7.86E-01	±	5.73E-01
^{207}Pb	(n,n)	^{207}Pb	(n,n)	7.14E-01	±	3.64E-01
^{241}Pu	Delayed Fission ν	^{241}Pu	Delayed Fission ν	6.81E-01	±	2.34E-03
			β_{eff} total uncertainty (%) =	6.82E+00	±	1.12E+00

As is listed in Table 3, elastic and inelastic reactions have a major impact on the β_{eff} uncertainty value. They are also noticeable the delayed fission ν and the total fission χ in ^{239}Pu and ^{240}Pu, respectively, and the induced fission and capture in ^{238}U. It is important to remark, however, that the JEFF-3.3 library does not contain covariance matrices for the delayed fission ν of relevant isotopes (^{239}Pu, ^{240}Pu, ^{238}U), and hence this contribution to the uncertainty is underestimated.

As it was done for the case of k_{eff}, the statistical error of the total uncertainty in β_{eff} has been also estimated as the standard deviation of eight Monte Carlo calculations with different random numbers sequences. The result obtained is:

$$\beta_{eff} \text{ total uncertainty (\%)} = 6.39 \pm 0.52$$

In this case the statistical errors of the total uncertainty are not so similar as in the k_{eff} case but they are still comparable in the order of magnitude.

Furthermore, the statistical error of some of the reactions with the highest contribution to the uncertainty has been analysed by this methodology:

[^{56}Fe(n,n) - ^{56}Fe(n,n)] uncertainty contribution (%) = 3.60 ± 0.77
[^{57}Fe(n,n) - ^{57}Fe(n,n)] uncertainty contribution (%) = 2.17 ± 0.53
[^{238}U(n,n) – ^{238}U(n,n')] uncertainty contribution (%) = -0.15 ± 1.44

Notice that in the first two cases, the statistical uncertainties obtained with this methodology are about half of those listed in Table 3, in the third case being essentially similar. The main uncertainty contributions depend on the elastic or inelastic reactions in structural materials, coolant and fuel.

Table 4. ISC for the major contributions to the β_{eff} uncertainty due to nuclear data. ISC obtained with MCNP(JEFF-3.3.)+SUMMON using Brestcher's approximation.

Quantity		β_{ISC}		
^{209}Bi	Elastic	-1.068E+00	±	8.199E-01
^{16}O	Elastic	-8.849E-01	±	5.738E-01
^{56}Fe	Elastic	-8.437E-01	±	6.043E-01
^{58}Ni	Elastic	6.888E-01	±	2.967E-01
^{239}Pu	Prompt Fission ν	-5.751E-01	±	1.795E-01
^{240}Pu	Elastic	5.450E-01	±	1.935E-01
^{239}Pu	Delayed Fission ν	3.930E-01	±	1.386E-03
^{238}U	Inelastic	3.740E-01	±	1.877E-01
^{238}U	Delayed Fission ν	3.187E-01	±	2.440E-03
^{208}Pb	Elastic	2.959E-01	±	5.317E-01

Calculations were performed again to achieve a nearer value to 1 pcm for the β_{eff} uncertainty and check if the impact of inelastic and elastic reactions decrease.

$$\beta_{eff} = 338.8 \pm 1.4 \text{ pcm}$$

The impact of these reactions (elastic and inelastic) decreases in some cases but still very significative. This likely means a lack of convergence due to a need for more statistic, especially for elastic and inelastic reactions.

[^{56}Fe(n,n) - ^{56}Fe(n,n)] uncertainty contribution (%) = 2.20 ± 0.69
[^{57}Fe(n,n) - ^{57}Fe(n,n)] uncertainty contribution (%) = 0.70 ± 0.32
[^{238}U(n,n) – ^{238}U(n,n')] uncertainty contribution (%) = -0.43 ± 0.41

3.2.2. Chiba's method

Chiba's method is known to be better in terms of decreasing the statistical uncertainty of the effective delayed neutron fraction and its sensitivities [Iwamoto, 2018]. The same reference was consulted to choose the scaling factor ($a = 20$) in order to keep the statistical effects sufficiently small.

The β_{eff} obtained using Chiba's method is:

$$\beta_{eff} = 332.2 \pm 0.2 \text{ pcm}$$

Table 5. Reactions with the largest contributions to the uncertainty in the effective delayed neutron fraction of the MYRRHA homogenized model calculated with MCNP+KSEN2sdf+SUMMON with JEFF-3.3 library using Chiba's method.

MYRRHA - JEFF-3.3						
Quantity				β_{eff} uncertainty (%)		
^{241}Pu	Delayed Fission ν	^{241}Pu	Delayed Fission ν	6.99E-01	±	1.06E-03
^{239}Pu	Total Fission χ	^{239}Pu	Total Fission χ	6.16E-01	±	6.07E-02
^{238}U	(n,f)	^{238}U	(n,f)	4.71E-01	±	6.74E-03
^{238}U	(n,n')	^{238}U	(n,f)	-3.92E-01	±	5.91E-03
^{241}Pu	Total Fission χ	^{241}Pu	Total Fission χ	3.62E-01	±	2.50E-02
^{238}U	(n,n)	^{238}U	(n,f)	3.22E-01	±	4.67E-03
^{240}Pu	(n,f)	^{240}Pu	(n,f)	2.80E-01	±	1.44E-02
^{239}Pu	Prompt Fission ν	^{239}Pu	Prompt Fission ν	2.64E-01	±	4.48E-03
^{238}U	(n,n')	^{238}U	(n,n')	2.59E-01	±	7.62E-02
^{238}U	(n,n)	^{238}U	(n,n')	-2.44E-01	±	6.91E-02
^{56}Fe	(n,n)	^{56}Fe	(n,n)	1.51E-01	±	1.06E-01
^{57}Fe	(n,n)	^{57}Fe	(n,n)	1.43E-01	±	5.64E-02
^{238}U	(n,n')	^{238}U	(n,γ)	1.40E-01	±	6.35E-03
^{238}U	Total Fission χ	^{238}U	Total Fission χ	1.38E-01	±	1.45E-02
^{241}Pu	(n,n)	^{241}Pu	(n,n)	1.31E-01	±	8.48E-02
^{238}U	(n,n)	^{238}U	(n,n)	1.26E-01	±	6.49E-02
^{238}U	Prompt Fission ν	^{238}U	Prompt Fission ν	1.26E-01	±	1.97E-03
^{54}Fe	(n,n)	^{54}Fe	(n,n)	1.14E-01	±	5.07E-02
^{238}Pu	Delayed Fission ν	^{238}Pu	Delayed Fission ν	1.12E-01	±	1.59E-04
^{209}Bi	(n,n')	^{209}Bi	(n,n')	9.67E-02	±	1.70E-02
			β_{eff} total uncertainty (%) =	1.26E+00	±	3.68E-02

It can be easily noted comparing Tables 4 and 6 that uncertainties have been reduced, especially in the case of elastic and inelastic reactions, and, as expected, the delayed fission ν and other fission-related data have the highest impact on the total uncertainty. In any case, it is important to remark, again that the JEFF-3.3 library does not contain covariance matrices for the delayed fission ν of relevant isotopes (^{239}Pu, ^{240}Pu, ^{238}U), and again this figure uncertainty is likely to be underestimated.

The total uncertainty of the β_{eff} was also calculated with an estimation using different random seeds in five MCNP calculations and the result obtained was:

$$\beta_{eff} \text{ total uncertainty (\%)} = 1.168 \pm 0.038$$

To conclude, Chiba's method allows to perform more precise calculations with less computational resources.

Table 6. ISC for the major contributions to the β_{eff} uncertainty due to nuclear data. ISC obtained with MCNP(JEFF-3.3.)+SUMMON using Chiba's method.

Quantity		β_{ISC}		
^{239}Pu	Prompt Fission ν	-5.859E-01	±	0.000E+00
^{239}Pu	Delayed Fission ν	4.001E-01	±	2.350E-03
^{238}U	Delayed Fission ν	3.052E-01	±	1.345E-03
^{238}U	Fission	1.976E-01	±	4.890E-03
^{239}Pu	Total Fission ν	-1.857E-01	±	2.105E-02
^{238}U	Total Fission ν	1.763E-01	±	4.680E-03
^{239}Pu	Fission	-1.679E-01	±	2.054E-02
^{241}Pu	Delayed Fission ν	1.404E-01	±	1.034E-03
^{238}U	Prompt Fission ν	-1.289E-01	±	4.347E-06
^{240}Pu	Prompt Fission ν	-1.199E-01	±	2.386E-05

3.3. VOID REACTIVITY WORTH

In this subsection, four different void scenarios have been considered for the void reactivity worth calculation. They have been proposed by SCK CEN based on studies [Hernandez-Solis, 2021] and [Barale, 2020] for a previous version of the MYRRHA model (v1.6). In the named "Void Scenario 0", the void formation is restricted to the central material testing IPS volume, then, the void expands radially towards the three next concentrical rings as is shown in Figure 3. The void scenario with the void formation affecting not only the central material testing IPS but also up to the first ring of fuel elements will be called "Void Scenario 1"; the void scenario with the void formation up to the second ring of fuel elements will be called "Void Scenario 2" and, lastly, the void scenario with the void formation up to the third ring of fuel elements will be called "Void Scenario 3".

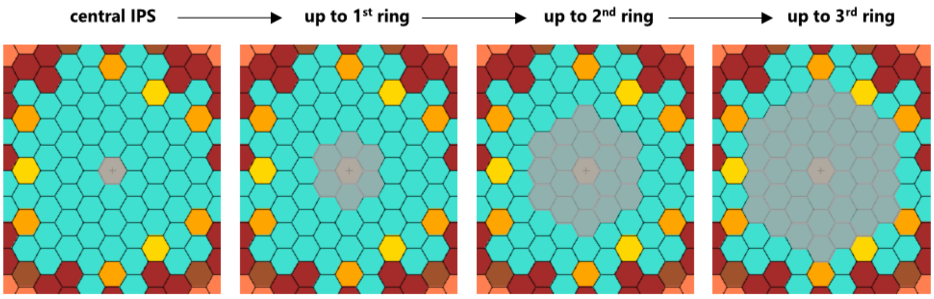

Figure 3. Void scenario configurations [Fiorito, 2021].

For these four void configurations, three void heights will be employed leading to twelve different scenarios. The void reactivity worth of all twelve scenarios is presented in Table 7. All scenarios were simulated by subtracting the coolant materials from the void volumes.

The small reactivity effect in the "Void Scenario 0" is insufficient to make an assumption about the behaviour of the void reactivity worth for 18 and 34 cm of void height, given the statistical precision of our calculations. For 72 cm of void height, when the reflectors are near to be reached or already reached by the void formation, the rise -in absolute value- of the void reactivity worth is more apparent. Void Scenario 1 was analysed in more detail for a better understanding of the void worth trend with the void height. As it is presented in Figure 4, the void worth rises slightly until it reaches its peak value at around 38-40 cm of void height, then it steadily decreases. The behaviour is similar in Void Scenario 2 as it can be seen in Figure 5 but with a higher void worth absolute value. Void Scenario 3 shows a different tendency in the void worth as is presented in Figure 6. When the void height starts to increase the void worth value rapidly increases and then when the peak value is reached at around 56 cm of void height the decrease is slighter than the fall of the other scenarios. Notice that all figures present error bars but it is more difficult to appreciate them in Void Scenarios 2 and 3.

Table 7. Void reactivity worth. Four radial configurations and three void heights.

VOID coefficient (ρ)			
	-9 to 9	**-17 to 17**	**-36 to 36**
vh (cm) =	**18**	**34**	**72**
Scenario 0 - IPS	11 ± 4	5 ± 4	-39 ± 4
Scenario 1 - First ring	170 ± 4	247 ± 4	-92 ± 4
Scenario 2 - Second ring	367 ± 4	512 ± 4	-381 ± 4
Scenario 3 - Third ring	1437 ± 4	3035 ± 4	3242 ± 4

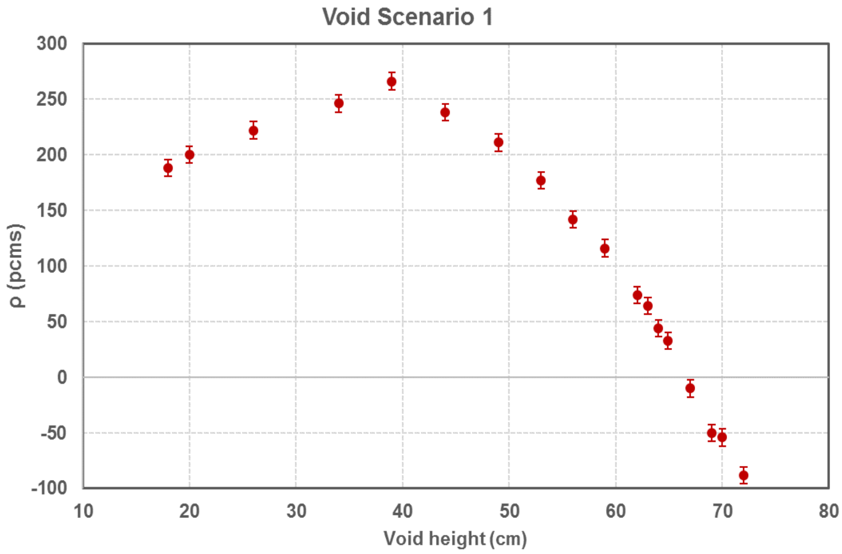

Figure 4. Void worth values for different void heights in Void Scenario 1.

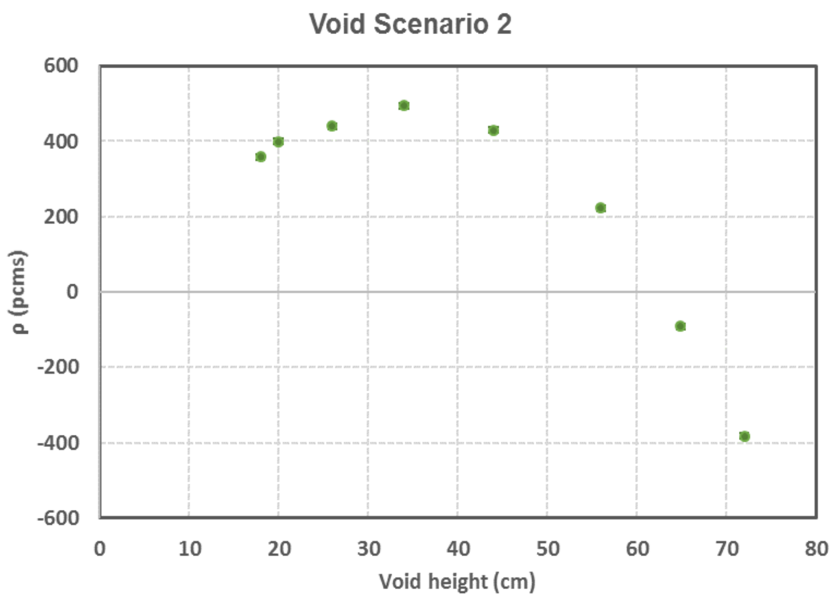

Figure 5. Void worth values for different void heights in Void Scenario 2.

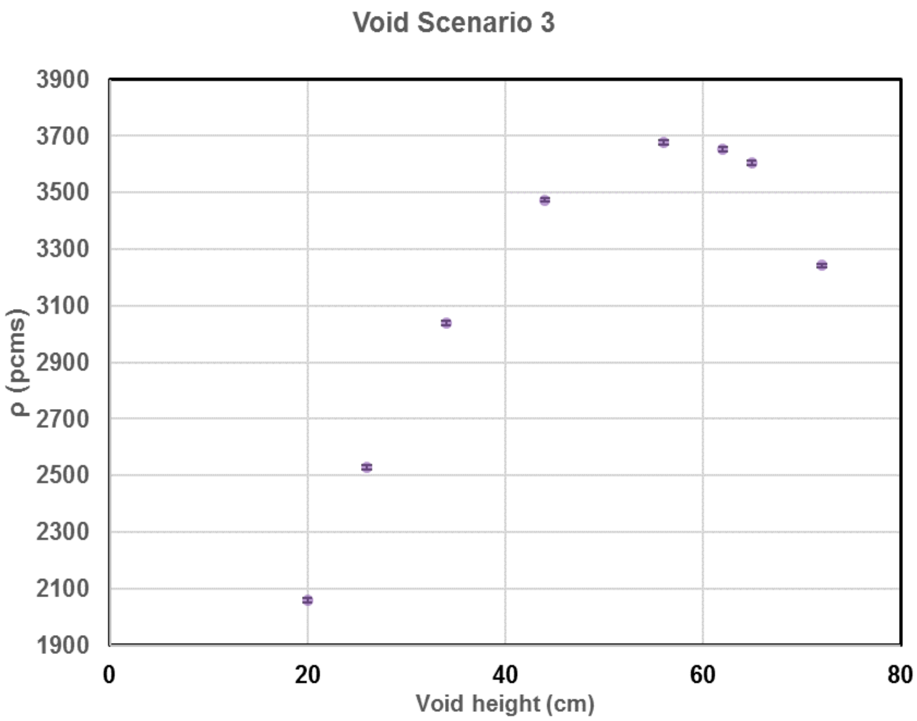

Figure 6. Void worth values for different void heights in Void Scenario 3

3.3.1. Void Scenario 0. Central IPS.

The main contributions to the uncertainty of the void worth value in Void Scenario 0 are shown in Table 8, Table 9 and Table 10, for void heights of 18 cm, 34 cm and 72 cm, respectively. It can be observed that the largest contributions are elastic and inelastic reactions in elements of the fuel, coolant and structural materials, such as O, Mn, Fe, Ni, Pb, U and Pu. When the void height starts to increase it also emerges as noticeable the impact of the total fission χ in the isotopes ^{239}Pu and ^{241}Pu. As mentioned above, relative uncertainties are notably high in this particular scenario, which is due to the small difference between the nominal and perturbed cases. For this reason, these results show very high uncertainties and the error in the contributions to the uncertainty of the individual reactions is largely consistent with zero, at least for the two lower void heights.

Table 8. Reactions with the largest contributions to the uncertainty in the void worth value of the MYRRHA homogenized model in Void Scenario 0 (void in central IPS) with 18 cm of void height calculated with MCNP+KSEN2sdf+SUMMON with JEFF-3.3 library.

MYRRHA - JEFF-3.3 - VOID SCENARIO 0 – Void height (-9 cm, 9 cm)						
Quantity				ρ uncertainty (%)		
^{56}Fe	(n,n)	^{56}Fe	(n,n)	8.97E+01	±	5.11E+01
^{57}Fe	(n,n)	^{57}Fe	(n,n)	7.39E+01	±	3.66E+01
^{238}U	(n,n')	^{238}U	(n,n')	6.01E+01	±	3.93E+01
^{16}O	(n,n)	^{16}O	(n,n)	5.96E+01	±	4.05E+01
^{54}Fe	(n,n)	^{54}Fe	(n,n)	5.50E+01	±	3.46E+01
^{58}Ni	(n,n)	^{58}Ni	(n,n)	4.22E+01	±	2.04E+01
^{238}U	(n,n)	^{238}U	(n,n')	-3.93E+01	±	3.28E+01
^{208}Pb	(n,n)	^{208}Pb	(n,n)	3.63E+01	±	3.61E+01
^{55}Mn	(n,n)	^{55}Mn	(n,n)	3.25E+01	±	2.97E+01
^{62}Ni	(n,n)	^{62}Ni	(n,n)	2.99E+01	±	1.88E+01
^{240}Pu	(n,n)	^{240}Pu	(n,n)	2.77E+01	±	1.97E+01
^{206}Pb	(n,n')	^{206}Pb	(n,n')	2.44E+01	±	2.12E+01
^{240}Pu	(n,n)	^{240}Pu	(n,n')	-2.27E+01	±	5.82E+01
^{238}U	Total Fission χ	^{238}U	Total Fission χ	2.08E+01	±	8.62E+00
^{241}Pu	(n,n')	^{241}Pu	(n,n')	2.04E+01	±	1.09E+01
^{58}Fe	(n,n)	^{58}Fe	(n,n)	1.97E+01	±	1.16E+01
^{24}Mg	(n,n)	^{24}Mg	(n,n)	1.91E+01	±	2.21E+01
^{206}Pb	(n,n)	^{206}Pb	(n,n)	1.84E+01	±	7.62E+00
^{238}U	(n,n')	^{238}U	(n,f)	-1.83E+01	±	1.83E+01
^{238}U	(n,n)	^{238}U	(n,n)	1.70E+01	±	3.63E+01
			ρ total uncertainty (%) =	1.82E+02	±	3.74E+01

Table 9. Reactions with the largest contributions to the uncertainty in the void worth value of the MYRRHA homogenized model in Void Scenario 0 (void in central IPS) with 34 cm of void height calculated with MCNP+KSEN2sdf+SUMMON with JEFF-3.3 library.

MYRRHA - JEFF-3.3 - VOID SCENARIO 0 – Void height (-17 cm, 17 cm)						
Quantity				ρ uncertainty (%)		
^{56}Fe	(n,n)	^{56}Fe	(n,n)	4.18E+02	±	2.01E+02
^{16}O	(n,n)	^{16}O	(n,n)	1.57E+02	±	1.13E+02
^{241}Pu	(n,n)	^{241}Pu	(n,n)	1.35E+02	±	1.59E+02
^{238}U	(n,n)	^{238}U	(n,n')	-1.29E+02	±	1.20E+02
^{238}U	(n,n')	^{238}U	(n,n')	1.24E+02	±	1.18E+02
^{57}Fe	(n,n)	^{57}Fe	(n,n)	1.18E+02	±	8.66E+01
^{240}Pu	(n,n)	^{240}Pu	(n,n')	-8.42E+01	±	9.18E+01
^{62}Ni	(n,n)	^{62}Ni	(n,n)	8.29E+01	±	6.21E+01
^{238}U	(n,n)	^{238}U	(n,n)	7.69E+01	±	1.11E+02
^{54}Fe	(n,n)	^{54}Fe	(n,n)	7.22E+01	±	4.22E+01
^{207}Pb	(n,n)	^{207}Pb	(n,n)	7.09E+01	±	5.92E+01
^{240}Pu	(n,n)	^{240}Pu	(n,n)	6.88E+01	±	4.96E+01
^{239}Pu	Total Fission χ	^{239}Pu	Total Fission χ	5.65E+01	±	8.97E+01
^{208}Pb	(n,n)	^{208}Pb	(n,n)	5.60E+01	±	7.47E+01
^{240}Pu	(n,n')	^{240}Pu	(n,n')	5.47E+01	±	6.05E+01
^{60}Ni	(n,n)	^{60}Ni	(n,n)	5.19E+01	±	4.63E+01
^{206}Pb	(n,n)	^{206}Pb	(n,n)	5.03E+01	±	3.32E+01
^{56}Fe	(n,n')	^{56}Fe	(n,n')	4.57E+01	±	3.85E+01
^{24}Mg	(n,n)	^{24}Mg	(n,n)	4.43E+01	±	5.18E+01
^{207}Pb	(n,n')	^{207}Pb	(n,n')	4.13E+01	±	3.26E+01
ρ total uncertainty (%)				5.41E+02	±	1.67E+02

Table 10. Reactions with the largest contributions to the uncertainty in the void worth value of the MYRRHA homogenized model in Void Scenario 0 (void in central IPS) with 72 cm of void height calculated with MCNP+KSEN2sdf+SUMMON with JEFF-3.3 library.

MYRRHA - JEFF-3.3 - VOID SCENARIO 0 – Void height (-36 cm, 36 cm)						
Quantity				ρ uncertainty (%)		
^{56}Fe	(n,n)	^{56}Fe	(n,n)	3.09E+01	±	1.58E+01
^{57}Fe	(n,n)	^{57}Fe	(n,n)	2.11E+01	±	6.79E+00
^{238}U	(n,n)	^{238}U	(n,n)	2.09E+01	±	1.05E+01
^{16}O	(n,n)	^{16}O	(n,n)	2.04E+01	±	9.90E+00
^{239}Pu	Total Fission χ	^{239}Pu	Total Fission χ	1.49E+01	±	1.09E+01
^{58}Ni	(n,n)	^{58}Ni	(n,n)	1.49E+01	±	5.20E+00
^{238}U	(n,n)	^{238}U	(n,n')	-1.42E+01	±	2.95E+01
^{241}Pu	(n,n)	^{241}Pu	(n,n)	1.33E+01	±	1.30E+01
^{241}Pu	(n,n')	^{241}Pu	(n,n')	1.32E+01	±	4.44E+00
^{240}Pu	(n,n)	^{240}Pu	(n,n)	1.10E+01	±	5.31E+00
^{55}Mn	(n,n)	^{55}Mn	(n,n)	9.98E+00	±	4.18E+00
^{208}Pb	(n,n)	^{208}Pb	(n,n)	9.58E+00	±	5.25E+00
^{53}Cr	(n,n)	^{53}Cr	(n,n)	9.25E+00	±	2.46E+00
^{58}Fe	(n,n)	^{58}Fe	(n,n)	7.81E+00	±	2.95E+00
^{54}Fe	(n,n)	^{54}Fe	(n,n)	7.79E+00	±	3.67E+00
^{207}Pb	(n,n)	^{207}Pb	(n,n)	7.41E+00	±	3.60E+00
^{206}Pb	(n,n)	^{206}Pb	(n,n)	6.91E+00	±	2.98E+00
^{241}Pu	Total Fission χ	^{241}Pu	Total Fission χ	6.81E+00	±	4.27E+00
^{206}Pb	(n,n)	^{206}Pb	(n,n')	6.54E+00	±	9.40E+00
^{25}Mg	(n,n)	^{25}Mg	(n,n)	6.52E+00	±	2.61E+00
ρ total uncertainty (%)				6.31E+01	±	1.21E+01

Table 11. ISC for the major contributions to the ρ_{VOID} uncertainty in Void Scenario 0 due to nuclear data. ISC obtained with MCNP(JEFF-3.3.)+SUMMON.

	Quantity		ρISC		
Void height = 18 cm	^{16}O	Elastic	3.093E+01	±	2.061E+01
	^{208}Pb	Elastic	1.655E+01	±	1.748E+01
	^{209}Bi	Elastic	1.333E+01	±	2.604E+01
	^{56}Fe	Elastic	1.173E+01	±	2.087E+01
	^{240}Pu	Elastic	-9.123E+00	±	6.099E+00
	^{238}U	Inelastic	-7.467E+00	±	6.425E+00
	^{54}Fe	Elastic	-7.424E+00	±	7.192E+00
	^{52}Cr	Elastic	-7.179E+00	±	8.480E+00
	^{206}Pb	Elastic	-6.867E+00	±	1.157E+01
	^{0}C	Elastic	6.174E+00	±	4.151E+00
Void height = 34 cm	^{56}Fe	Elastic	1.030E+02	±	5.705E+01
	^{16}O	Elastic	7.473E+01	±	5.754E+01
	^{209}Bi	Elastic	6.682E+01	±	7.563E+01
	^{238}U	Elastic	4.782E+01	±	5.199E+01
	^{207}Pb	Elastic	2.657E+01	±	3.709E+01
	^{52}Cr	Elastic	1.875E+01	±	2.069E+01
	^{208}Pb	Elastic	1.844E+01	±	4.249E+01
	^{238}U	Inelastic	-1.744E+01	±	1.616E+01
	^{206}Pb	Elastic	-1.540E+01	±	3.413E+01
	^{56}Fe	Inelastic	-1.439E+01	±	1.269E+01
Void height = 72 cm	^{16}O	Elastic	9.971E+00	±	5.054E+00
	^{209}Bi	Elastic	9.363E+00	±	6.934E+00
	^{238}U	Elastic	7.030E+00	±	4.888E+00
	^{56}Fe	Elastic	4.964E+00	±	5.437E+00
	^{240}Pu	Elastic	-3.375E+00	±	1.595E+00
	^{207}Pb	Elastic	3.283E+00	±	2.919E+00
	^{55}Mn	Elastic	2.455E+00	±	1.426E+00
	^{0}C	Elastic	2.035E+00	±	1.048E+00
	^{208}Pb	Elastic	1.881E+00	±	4.591E+00
	^{24}Mg	Elastic	-1.437E+00	±	1.253E+00

3.3.2. Void Scenario 1. IPS + 1st ring

Again, elastic and inelastic reactions are the ones having the highest impact, also in the same materials that were highlighted in Void Scenario 0 (O, Mn, Fe, Ni, Pb, U and Pu). In these scenarios, it is again noticeable the impact of the total fission χ in isotopes ^{239}Pu and ^{241}Pu, although these results are also affected by large statistical uncertainties. The total uncertainty due to nuclear data in these cases is around 14.5% with 18cm of void height, 10.6% with 34cm of height and 31.5% with 72cm of height.

Table 12. Reactions with the largest contributions to the uncertainty in the void worth value of the MYRRHA homogenized model in Void Scenario 1 (void in central IPS + 1st ring) with 18 cm of void height calculated with MCNP+KSEN2sdf+SUMMON with JEFF-3.3 library.

MYRRHA - JEFF-3.3 - VOID SCENARIO 1 – Void height (-9 cm, 9 cm)						
Quantity				ρ uncertainty (%)		
^{56}Fe	(n,n)	^{56}Fe	(n,n)	8.16E+00	±	4.43E+00
^{239}Pu	Total Fission χ	^{239}Pu	Total Fission χ	4.91E+00	±	2.32E+00
^{238}U	(n,n')	^{238}U	(n,n')	4.33E+00	±	2.77E+00
^{58}Ni	(n,n)	^{58}Ni	(n,n)	4.02E+00	±	1.56E+00
^{241}Pu	(n,n)	^{241}Pu	(n,n)	3.88E+00	±	3.02E+00
^{57}Fe	(n,n)	^{57}Fe	(n,n)	3.83E+00	±	1.72E+00
^{16}O	(n,n)	^{16}O	(n,n)	3.31E+00	±	2.33E+00
^{238}U	(n,n)	^{238}U	(n,n')	-2.94E+00	±	1.80E+00
^{54}Fe	(n,n)	^{54}Fe	(n,n)	2.30E+00	±	8.49E-01
^{238}U	(n,n')	^{238}U	(n,f)	-2.26E+00	±	5.86E-01
^{240}Pu	(n,n)	^{240}Pu	(n,n')	-2.11E+00	±	2.35E+00
^{56}Fe	(n,n')	^{56}Fe	(n,n')	2.07E+00	±	5.88E-01
^{58}Fe	(n,n)	^{58}Fe	(n,n)	1.96E+00	±	7.25E-01
^{55}Mn	(n,n)	^{55}Mn	(n,n)	1.91E+00	±	1.33E+00
^{206}Pb	(n,n')	^{206}Pb	(n,n')	1.90E+00	±	1.42E+00
^{238}U	(n,n')	^{238}U	(n,γ)	-1.79E+00	±	3.00E-01
^{206}Pb	(n,n)	^{206}Pb	(n,n)	1.79E+00	±	6.92E-01
^{240}Pu	(n,n)	^{240}Pu	(n,n)	1.75E+00	±	1.23E+00
^{208}Pb	(n,n)	^{208}Pb	(n,n)	1.59E+00	±	1.65E+00
^{241}Pu	Total Fission χ	^{241}Pu	Total Fission χ	1.59E+00	±	9.38E-01
			ρ total uncertainty (%) =	1.45E+01	±	2.96E+00

Table 13. Reactions with the largest contributions to the uncertainty in the void worth value of the MYRRHA homogenized model in Void Scenario 1 (void in central IPS + 1st ring) with 34 cm of void height calculated with MCNP+KSEN2sdf+SUMMON with JEFF-3.3 library.

MYRRHA - JEFF-3.3						
Quantity				ρ uncertainty (%)		
^{57}Fe	(n,n)	^{57}Fe	(n,n)	5.02E+00	±	1.58E+00
^{238}U	(n,n')	^{238}U	(n,n')	4.18E+00	±	1.81E+00
^{56}Fe	(n,n)	^{56}Fe	(n,n)	3.73E+00	±	2.04E+00
^{239}Pu	Total Fission χ	^{239}Pu	Total Fission χ	3.73E+00	±	1.53E+00
^{238}U	(n,n')	^{238}U	(n,f)	-2.29E+00	±	3.97E-01
^{206}Pb	(n,n')	^{206}Pb	(n,n')	2.14E+00	±	9.73E-01
^{58}Ni	(n,n)	^{58}Ni	(n,n)	2.06E+00	±	8.67E-01
^{238}U	(n,n)	^{238}U	(n,n')	2.02E+00	±	8.51E-01
^{16}O	(n,n)	^{16}O	(n,n)	1.97E+00	±	1.65E+00
^{207}Pb	(n,n')	^{207}Pb	(n,n')	1.73E+00	±	6.19E-01
^{55}Mn	(n,n)	^{55}Mn	(n,n)	1.68E+00	±	1.16E+00
^{238}U	(n,n')	^{238}U	(n,γ)	-1.64E+00	±	1.91E-01
^{60}Ni	(n,n)	^{60}Ni	(n,n)	1.55E+00	±	9.55E-01
^{54}Fe	(n,n)	^{54}Fe	(n,n)	1.53E+00	±	8.25E-01
^{208}Pb	(n,n)	^{208}Pb	(n,n)	1.52E+00	±	1.90E+00
^{62}Ni	(n,n)	^{62}Ni	(n,n)	1.38E+00	±	7.97E-01
^{27}Al	(n,n)	^{27}Al	(n,n)	1.29E+00	±	6.31E-01
^{239}Pu	(n,f)	^{239}Pu	(n,f)	1.28E+00	±	2.31E-01
^{241}Pu	Total Fission χ	^{241}Pu	Total Fission χ	1.18E+00	±	6.45E-01
^{206}Pb	(n,n)	^{206}Pb	(n,n')	-1.12E+00	±	4.80E-01
			ρ total uncertainty (%) =	1.06E+01	±	1.58E+00

Table 14. Reactions with the largest contributions to the uncertainty in the void worth value of the MYRRHA homogenized model in Void Scenario 1 (void in central IPS + 1st ring) with 72 cm of void height calculated with MCNP+KSEN2sdf+SUMMON with JEFF-3.3 library.

MYRRHA - JEFF-3.3						
Quantity				ρ uncertainty (%)		
^{56}Fe	(n,n)	^{56}Fe	(n,n)	1.40E+01	±	7.72E+00
^{16}O	(n,n)	^{16}O	(n,n)	1.37E+01	±	4.36E+00
^{239}Pu	Total Fission χ	^{239}Pu	Total Fission χ	1.24E+01	±	4.40E+00
^{238}U	(n,n')	^{238}U	(n,n')	1.18E+01	±	5.22E+00
^{238}U	(n,n)	^{238}U	(n,n')	-1.10E+01	±	4.79E+00
^{57}Fe	(n,n)	^{57}Fe	(n,n)	9.68E+00	±	3.75E+00
^{238}U	(n,n')	^{238}U	(n,f)	-8.32E+00	±	8.29E-01
^{55}Mn	(n,n)	^{55}Mn	(n,n)	7.30E+00	±	3.66E+00
^{238}U	(n,n)	^{238}U	(n,f)	7.12E+00	±	6.98E-01
^{238}U	(n,n')	^{238}U	(n,γ)	-6.28E+00	±	5.39E-01
^{238}U	(n,n)	^{238}U	(n,n)	5.99E+00	±	4.20E+00
^{206}Pb	(n,n')	^{206}Pb	(n,n')	5.68E+00	±	2.49E+00
^{238}U	(n,f)	^{238}U	(n,f)	4.83E+00	±	4.70E-01
^{208}Pb	(n,n)	^{208}Pb	(n,n)	4.70E+00	±	3.54E+00
^{240}Pu	(n,n)	^{240}Pu	(n,n)	4.04E+00	±	2.28E+00
^{241}Pu	Total Fission χ	^{241}Pu	Total Fission χ	3.99E+00	±	1.68E+00
^{207}Pb	(n,n')	^{207}Pb	(n,n')	3.87E+00	±	1.76E+00
^{238}U	(n,n')	^{238}U	(n,2n)	-3.81E+00	±	1.44E+00
^{58}Ni	(n,n)	^{58}Ni	(n,n)	3.79E+00	±	2.07E+00
^{240}Pu	(n,f)	^{240}Pu	(n,f)	3.71E+00	±	1.01E+00
			ρ total uncertainty (%) =	3.15E+01	±	4.78E+00

Table 15. ISC for the major contributions to the ρ_{VOID} uncertainty in Void Scenario 1 due to nuclear data. ISC obtained with MCNP(JEFF-3.3.)+SUMMON.

	Quantity		ρISC		
Void height = 18 cm	^{56}Fe	Elastic	2.104E+00	±	1.234E+00
	^{209}Bi	Elastic	1.978E+00	±	1.561E+00
	^{16}O	Elastic	1.438E+00	±	1.196E+00
	^{239}Pu	Total Fission ν	-1.228E+00	±	3.572E-01
	^{239}Pu	Prompt Fission ν	-1.224E+00	±	3.558E-01
	^{239}Pu	Fission	-9.213E-01	±	3.645E-01
	^{58}Ni	Elastic	-9.079E-01	±	5.579E-01
	^{207}Pb	Elastic	7.678E-01	±	6.580E-01
	^{56}Fe	Inelastic	-6.653E-01	±	1.986E-01
	^{240}Pu	Elastic	-6.572E-01	±	3.786E-01
Void height = 34 cm	^{239}Pu	Total Fission ν	-1.339E+00	±	2.480E-01
	^{239}Pu	Prompt Fission ν	-1.334E+00	±	2.471E-01
	^{209}Bi	Elastic	1.240E+00	±	1.062E+00
	^{239}Pu	Fission	-1.065E+00	±	2.520E-01
	^{16}O	Elastic	9.411E-01	±	8.434E-01
	^{208}Pb	Elastic	6.800E-01	±	7.044E-01
	^{56}Fe	Elastic	6.123E-01	±	8.265E-01
	^{238}U	Inelastic	-5.933E-01	±	2.531E-01
	^{238}U	Total Fission ν	5.492E-01	±	5.692E-02
	^{238}U	Prompt Fission ν	5.427E-01	±	5.609E-02
Void height = 72 cm	^{16}O	Elastic	6.759E+00	±	2.232E+00
	^{209}Bi	Elastic	5.782E+00	±	2.806E+00
	^{56}Fe	Elastic	4.332E+00	±	2.369E+00
	^{238}U	Total Fission ν	2.439E+00	±	1.644E-01
	^{238}U	Prompt Fission ν	2.403E+00	±	1.624E-01
	^{239}Pu	Total Fission ν	-2.008E+00	±	6.588E-01
	^{239}Pu	Prompt Fission ν	-2.002E+00	±	6.543E-01
	^{238}U	Inelastic	-1.772E+00	±	7.102E-01
	^{238}U	(n,γ)	1.709E+00	±	1.044E-01

3.3.3. Void Scenario 2. IPS + 1st and 2nd ring

Following the trend of Void Scenarios 0 and 1, in Void Scenario 2 elastic and inelastic reactions are still the major contributors to the void worth value uncertainty, as well as the total fission χ reaction in isotope ^{239}Pu that was already mentioned above in Void Scenario 1. In this case, however, ^{238}U fission and capture reactions also begin to become important. Captures in plutonium isotopes also have a higher relative impact in Void Scenario 2. For a void height of 34cm, it is also noticeable the impact of prompt fission ν for ^{239}Pu. As it is listed in Table 16, Table 17 and Table 18, the total contributions due to nuclear data for void heights of 18, 34 and 72 cm are around 8%, 8% and 13%, respectively.

Table 16. Reactions with the largest contributions to the uncertainty in the void worth value of the MYRRHA homogenized model in Void Scenario 2 (void in central IPS + 1st and 2nd ring) with 18 cm of void height calculated with MCNP+KSEN2sdf+SUMMON with JEFF-3.3 library.

MYRRHA - JEFF-3.3						
Quantity				ρ uncertainty (%)		
^{56}Fe	(n,n)	^{56}Fe	(n,n)	3.51E+00	±	1.69E+00
^{238}U	(n,n)	^{238}U	(n,n)	3.24E+00	±	1.12E+00
^{238}U	(n,n)	^{238}U	(n,n')	-3.12E+00	±	2.35E+00
^{239}Pu	Total Fission χ	^{239}Pu	Total Fission χ	2.80E+00	±	1.07E+00
^{238}U	(n,n)	^{238}U	(n,f)	2.43E+00	±	2.74E-01
^{206}Pb	(n,n')	^{206}Pb	(n,n')	2.12E+00	±	6.65E-01
^{238}U	(n,n')	^{238}U	(n,n')	1.70E+00	±	1.05E+00
^{16}O	(n,n)	^{16}O	(n,n)	1.66E+00	±	1.08E+00
^{238}U	(n,n')	^{238}U	(n,f)	-1.52E+00	±	1.72E-01
^{58}Ni	(n,n)	^{58}Ni	(n,n)	1.50E+00	±	6.50E-01
^{209}Bi	(n,n')	^{209}Bi	(n,n')	1.47E+00	±	2.85E-01
^{239}Pu	(n,f)	^{239}Pu	(n,f)	1.37E+00	±	1.47E-01
^{57}Fe	(n,n)	^{57}Fe	(n,n)	1.34E+00	±	5.62E-01
^{54}Fe	(n,n)	^{54}Fe	(n,n)	1.32E+00	±	5.71E-01
^{208}Pb	(n,n)	^{208}Pb	(n,n)	1.28E+00	±	7.98E-01
^{207}Pb	(n,n')	^{207}Pb	(n,n')	1.24E+00	±	4.58E-01
^{240}Pu	(n,n)	^{240}Pu	(n,n')	1.21E+00	±	1.19E+00
^{240}Pu	(n,n)	^{240}Pu	(n,n)	1.12E+00	±	5.57E-01
^{238}U	(n,n)	^{238}U	(n,γ)	1.03E+00	±	1.29E-01
^{238}U	(n,f)	^{238}U	(n,f)	1.02E+00	±	1.15E-01
			ρ total uncertainty (%) =	8.11E+00	±	1.25E+00

Table 17. Reactions with the largest contributions to the uncertainty in the void worth value of the MYRRHA homogenized model in Void Scenario 2 (void in central IPS + 1st and 2nd ring) with 34 cm of void height calculated with MCNP+KSEN2sdf+SUMMON with JEFF-3.3 library.

MYRRHA – JEFF-3.3						
Quantity				ρ uncertainty (%)		
^{56}Fe	(n,n)	^{56}Fe	(n,n)	3.88E+00	±	1.40E+00
^{239}Pu	Total Fission χ	^{239}Pu	Total Fission χ	3.31E+00	±	7.78E-01
^{238}U	(n,n')	^{238}U	(n,n')	2.50E+00	±	8.76E-01
^{206}Pb	(n,n')	^{206}Pb	(n,n')	2.39E+00	±	5.16E-01
^{238}U	(n,n')	^{238}U	(n,f)	-2.32E+00	±	1.27E-01
^{209}Bi	(n,n')	^{209}Bi	(n,n')	1.80E+00	±	2.20E-01
^{16}O	(n,n)	^{16}O	(n,n)	1.67E+00	±	8.35E-01
^{238}U	(n,f)	^{238}U	(n,f)	1.57E+00	±	8.46E-02
^{239}Pu	(n,f)	^{239}Pu	(n,f)	1.57E+00	±	1.07E-01
^{57}Fe	(n,n)	^{57}Fe	(n,n)	1.54E+00	±	5.43E-01
^{238}U	(n,n')	^{238}U	(n,γ)	-1.51E+00	±	5.97E-02
^{58}Ni	(n,n)	^{58}Ni	(n,n)	1.49E+00	±	5.66E-01
^{241}Pu	(n,n)	^{241}Pu	(n,n)	1.45E+00	±	1.02E+00
^{207}Pb	(n,n')	^{207}Pb	(n,n')	1.41E+00	±	3.46E-01
^{206}Pb	(n,n)	^{206}Pb	(n,n')	-1.15E+00	±	2.38E-01
^{238}U	(n,n)	^{238}U	(n,n')	1.13E+00	±	3.94E-01
^{238}U	(n,γ)	^{238}U	(n,γ)	1.08E+00	±	2.57E-02
^{241}Pu	Total Fission χ	^{241}Pu	Total Fission χ	9.96E-01	±	3.32E-01
^{56}Fe	(n,n')	^{56}Fe	(n,n')	9.56E-01	±	2.25E-01
^{208}Pb	(n,n')	^{208}Pb	(n,n')	8.68E-01	±	1.66E-01
			ρ total uncertainty (%) =	7.96E+00	±	9.01E-01

As it was done for the case of k_{eff} and β_{eff}, in this particular scenario the statistical error of the total uncertainty in ρ has been also estimated as the standard deviation of several (eight) Monte Carlo calculations with different random numbers sequences. The result obtained is:

$$\rho_{VOID} \text{ total uncertainty (\%)} = 5.95 \pm 0.66$$

In this case, the value obtained in this way is about 2-σ below the value listed in Table 17. Furthermore, some of the reactions with high contribution to the uncertainty were analysed by this methodology:

[^{56}Fe(n,n) - ^{56}Fe(n,n)] uncertainty contribution (%) = 2.64 ± 0.82
[^{239}Pu (Total Fission χ) -^{239}Pu (Total Fission χ)] uncertainty contribution (%) = 2.34 ± 0.57
[^{238}U(n,n) – ^{238}U(n,n)] uncertainty contribution (%) = 0.98 ± 0.19
[^{238}U(n,f) – ^{238}U(n,f)] uncertainty contribution (%) = 1.56 ± 0.10
[^{239}Pu(n,f) – ^{239}Pu(n,f)] uncertainty contribution (%) = 1.46 ± 0.08

In the first case, the error estimate is about half the one provided by SUMMON and listed in Table 17, the second case being similar. The third case is not consistent with SUMMON results but being the case of a scattering reaction could be due to a lack of convergence and a need for more statistic. Again, further studies will be needed for understanding this behaviour. Fourth and fifth cases are also consistent with SUMMON results in Table 17.

Table 18. Reactions with the largest contributions to the uncertainty in the void worth value of the MYRRHA homogenized model in Void Scenario 2 (void in central IPS + 1st and 2nd ring) with 72 cm of void height calculated with MCNP+KSEN2sdf+SUMMON with JEFF-3.3 library.

MYRRHA - JEFF-3.3						
Quantity				ρ uncertainty (%)		
^{239}Pu	Total Fission χ	^{239}Pu	Total Fission χ	7.02E+00	±	1.02E+00
^{206}Pb	(n,n')	^{206}Pb	(n,n')	4.54E+00	±	6.10E-01
^{238}U	(n,n')	^{238}U	(n,f)	-4.30E+00	±	1.41E-01
^{238}U	(n,n')	^{238}U	(n,n')	3.82E+00	±	1.07E+00
^{238}U	(n,f)	^{238}U	(n,f)	3.55E+00	±	1.15E-01
^{56}Fe	(n,n)	^{56}Fe	(n,n)	3.25E+00	±	1.24E+00
^{209}Bi	(n,n')	^{209}Bi	(n,n')	3.10E+00	±	2.65E-01
^{240}Pu	(n,f)	^{240}Pu	(n,f)	2.68E+00	±	2.33E-01
^{16}O	(n,n)	^{16}O	(n,n)	2.57E+00	±	1.02E+00
^{240}Pu	(n,f)	^{240}Pu	(n,γ)	2.50E+00	±	5.23E-02
^{238}U	(n,n')	^{238}U	(n,γ)	-2.35E+00	±	7.93E-02
^{241}Pu	Total Fission χ	^{241}Pu	Total Fission χ	2.26E+00	±	4.26E-01
^{207}Pb	(n,n')	^{207}Pb	(n,n')	1.99E+00	±	4.11E-01
^{238}U	(n,γ)	^{238}U	(n,γ)	1.84E+00	±	3.47E-02
^{238}U	(n,n)	^{238}U	(n,f)	1.79E+00	±	5.83E-02
^{206}Pb	(n,n)	^{206}Pb	(n,n')	1.76E+00	±	2.47E-01
^{238}U	(n,f)	^{238}U	(n,γ)	-1.70E+00	±	6.38E-02
^{241}Pu	(n,n)	^{241}Pu	(n,n)	1.68E+00	±	1.35E+00
^{238}U	(n,n)	^{238}U	(n,n')	-1.67E+00	±	4.17E-01
^{239}Pu	(n,f)	^{239}Pu	(n,f)	1.66E+00	±	1.12E-01
			ρ total uncertainty (%) =	1.28E+01	±	8.32E-01

Table 19. ISC for the major contributions to the ρ_{VOID} uncertainty in Void Scenario 2 due to nuclear data. ISC obtained with MCNP(JEFF-3.3.)+SUMMON.

	Quantity		ρISC		
Void height = 18 cm	^{239}Pu	Total Fission ν	-1.412E+00	±	1.648E-01
	^{239}Pu	Prompt Fission ν	-1.408E+00	±	1.641E-01
	^{239}Pu	Fission	-1.119E+00	±	1.676E-01
	^{238}U	Elastic	1.081E+00	±	5.137E-01
	^{16}O	Elastic	7.976E-01	±	5.488E-01
	^{238}U	Total Fission ν	5.712E-01	±	3.673E-02
	^{238}U	Prompt Fission ν	5.634E-01	±	3.622E-02
	^{238}U	(n,γ)	5.337E-01	±	2.404E-02
	^{56}Fe	Elastic	3.928E-01	±	5.726E-01
	^{52}Cr	Elastic	-3.647E-01	±	2.296E-01
Void height = 34 cm	^{209}Bi	Elastic	9.478E-01	±	5.309E-01
	^{16}O	Elastic	8.682E-01	±	4.259E-01
	^{238}U	Total Fission ν	8.360E-01	±	2.818E-02
	^{238}U	Prompt Fission ν	8.241E-01	±	2.777E-02
	^{56}Fe	Elastic	7.799E-01	±	4.225E-01
	^{238}U	Capture	6.962E-01	±	1.782E-02
	^{238}U	Fission	4.852E-01	±	2.931E-02
	^{209}Bi	Inelastic	4.689E-01	±	5.248E-02
	^{208}Pb	Elastic	3.165E-01	±	3.520E-01
	^{239}Pu	Capture	2.954E-01	±	1.312E-02
Void height = 72 cm	^{238}U	Total Fission ν	1.791E+00	±	4.008E-02
	^{238}U	Prompt Fission ν	1.768E+00	±	3.959E-02
	^{16}O	Elastic	1.325E+00	±	5.227E-01
	^{239}Pu	Total Fission ν	-1.262E+00	±	1.643E-01
	^{239}Pu	Prompt Fission ν	-1.256E+00	±	1.637E-01
	^{238}U	Fission	1.153E+00	±	3.989E-02
	^{238}U	(n,γ)	1.150E+00	±	2.350E-02
	^{56}Fe	Elastic	8.034E-01	±	5.486E-01
	^{209}Bi	Inelastic	7.964E-01	±	6.118E-02
	^{240}Pu	Total Fission ν	6.382E-01	±	2.670E-02

3.3.4. Void scenario 3. IPS + 1st, 2nd and 3rd ring

In Void Scenario 3, the contribution of fission reactions in ^{239}Pu begins to increase, as well as prompt fission ν in this same isotope. The major remaining contributions are the same as the ones mentioned above in Void Scenario 2. However, with the increasing precision in the results there are two scattering reactions that appear to clearly dominate the uncertainty: ^{206}Pb (n,n’) and ^{238}U (n,n’). The total contribution in the void worth value due to nuclear data is around 2.0% for 18 cm of void height, 1.8% for 34 cm of void height and 2.2% for 72 cm of void height.

Table 20. Reactions with the largest contributions to the uncertainty in the void worth value of the MYRRHA homogenized model in Void Scenario 3 (void in central IPS + 1st, 2nd and 3rd ring) with 18 cm of void height calculated with MCNP+KSEN2sdf+SUMMON with JEFF-3.3 library.

MYRRHA - JEFF-3.3						
Quantity				ρ uncertainty (%)		
^{238}U	(n,n')	^{238}U	(n,n')	9.65E-01	±	2.42E-01
^{238}U	(n,n)	^{238}U	(n,n')	-8.06E-01	±	1.95E-01
^{239}Pu	Total Fission χ	^{239}Pu	Total Fission χ	6.51E-01	±	1.95E-01
^{206}Pb	(n,n')	^{206}Pb	(n,n')	6.40E-01	±	1.28E-01
^{239}Pu	(n,f)	^{239}Pu	(n,f)	6.31E-01	±	2.83E-02
^{56}Fe	(n,n)	^{56}Fe	(n,n)	5.98E-01	±	3.00E-01
^{238}U	(n,n')	^{238}U	(n,f)	-5.60E-01	±	4.76E-02
^{240}Pu	(n,f)	^{240}Pu	(n,f)	5.39E-01	±	4.94E-02
^{238}U	(n,n')	^{238}U	(n,γ)	-5.21E-01	±	1.91E-02
^{57}Fe	(n,n)	^{57}Fe	(n,n)	4.62E-01	±	1.45E-01
^{16}O	(n,n)	^{16}O	(n,n)	4.50E-01	±	2.05E-01
^{239}Pu	Prompt Fission ν	^{239}Pu	Prompt Fission ν	4.43E-01	±	1.48E-02
^{240}Pu	(n,f)	^{240}Pu	(n,γ)	-4.34E-01	±	1.21E-02
^{209}Bi	(n,n')	^{209}Bi	(n,n')	4.29E-01	±	5.35E-02
^{238}U	(n,n)	^{238}U	(n,f)	4.01E-01	±	3.48E-02
^{58}Ni	(n,n)	^{58}Ni	(n,n)	3.99E-01	±	1.18E-01
^{238}U	(n,n)	^{238}U	(n,n)	3.69E-01	±	2.05E-01
^{208}Pb	(n,n)	^{208}Pb	(n,n)	3.45E-01	±	2.57E-01
^{207}Pb	(n,n')	^{207}Pb	(n,n')	3.30E-01	±	8.31E-02
^{239}Pu	(n,γ)	^{239}Pu	(n,γ)	2.89E-01	±	1.53E-02
			ρ total uncertainty (%) =	2.02E+00	±	1.58E-01

Table 21. Reactions with the largest contributions to the uncertainty in the void worth value of the MYRRHA homogenized model in Void Scenario 3 (void in central IPS + 1st, 2nd and 3rd ring) with 34 cm of void height calculated with MCNP+KSEN2sdf+SUMMON with JEFF-3.3 library.

MYRRHA - JEFF-3.3						
Quantity				ρ uncertainty (%)		
^{206}Pb	(n,n')	^{206}Pb	(n,n')	7.85E-01	±	7.57E-02
^{238}U	(n,n')	^{238}U	(n,n')	6.65E-01	±	1.54E-01
^{239}Pu	(n,f)	^{239}Pu	(n,f)	6.28E-01	±	1.63E-02
^{239}Pu	Total Fission χ	^{239}Pu	Total Fission χ	5.65E-01	±	1.26E-01
^{240}Pu	(n,f)	^{240}Pu	(n,f)	5.43E-01	±	2.85E-02
^{238}U	(n,n)	^{238}U	(n,n')	-5.43E-01	±	1.20E-01
^{238}U	(n,n')	^{238}U	(n,f)	-4.93E-01	±	2.51E-02
^{209}Bi	(n,n')	^{209}Bi	(n,n')	4.69E-01	±	3.15E-02
^{239}Pu	Prompt Fission ν	^{239}Pu	Prompt Fission ν	4.51E-01	±	9.29E-03
^{240}Pu	(n,f)	^{240}Pu	(n,γ)	-4.42E-01	±	7.12E-03
^{238}U	(n,n')	^{238}U	(n,γ)	-4.15E-01	±	9.91E-03
^{56}Fe	(n,n)	^{56}Fe	(n,n)	3.72E-01	±	1.74E-01
^{208}Pb	(n,n)	^{208}Pb	(n,n)	3.56E-01	±	1.65E-01
^{238}U	(n,n)	^{238}U	(n,f)	3.46E-01	±	1.77E-02
^{206}Pb	(n,n)	^{206}Pb	(n,n')	3.42E-01	±	3.36E-02
^{207}Pb	(n,n')	^{207}Pb	(n,n')	3.05E-01	±	5.00E-02
^{239}Pu	(n,γ)	^{239}Pu	(n,γ)	3.03E-01	±	9.64E-03
^{238}U	(n,γ)	^{238}U	(n,γ)	2.92E-01	±	4.23E-03
^{238}U	(n,f)	^{238}U	(n,f)	2.73E-01	±	1.37E-02
^{239}Pu	(n,f)	^{239}Pu	(n,γ)	2.71E-01	±	6.76E-03
			ρ total uncertainty (%) =	1.82E+00	±	8.47E-02

Table 22. Reactions with the largest contributions to the uncertainty in the void worth value of the MYRRHA homogenized model in Void Scenario 3 (void in central IPS + 1st, 2nd and 3rd ring) with 72 cm of void height calculated with MCNP+KSEN2sdf+SUMMON with JEFF-3.3 library.

MYRRHA - JEFF-3.3						
Quantity				ρ uncertainty (%)		
^{206}Pb	(n,n')	^{206}Pb	(n,n')	9.06E-01	±	6.64E-02
^{238}U	(n,n')	^{238}U	(n,n')	8.83E-01	±	1.39E-01
^{239}Pu	Total Fission χ	^{239}Pu	Total Fission χ	7.41E-01	±	1.17E-01
^{238}U	(n,n')	^{238}U	(n,f)	-6.96E-01	±	2.37E-02
^{239}Pu	(n,f)	^{239}Pu	(n,f)	6.70E-01	±	1.47E-02
^{209}Bi	(n,n')	^{209}Bi	(n,n')	6.26E-01	±	2.77E-02
^{208}Pb	(n,n)	^{208}Pb	(n,n)	5.79E-01	±	1.46E-01
^{238}U	(n,n')	^{238}U	(n,γ)	-5.22E-01	±	8.70E-03
^{239}Pu	Prompt Fission ν	^{239}Pu	Prompt Fission ν	4.96E-01	±	8.22E-03
^{240}Pu	(n,f)	^{240}Pu	(n,f)	4.86E-01	±	2.67E-02
^{240}Pu	(n,f)	^{240}Pu	(n,γ)	-4.79E-01	±	5.41E-03
^{56}Fe	(n,n)	^{56}Fe	(n,n)	4.52E-01	±	1.75E-01
^{238}U	(n,f)	^{238}U	(n,f)	4.10E-01	±	1.36E-02
^{238}U	(n,γ)	^{238}U	(n,γ)	3.70E-01	±	3.55E-03
^{207}Pb	(n,n')	^{207}Pb	(n,n')	3.67E-01	±	4.17E-02
^{16}O	(n,n)	^{16}O	(n,n)	3.51E-01	±	1.20E-01
^{239}Pu	(n,f)	^{239}Pu	(n,γ)	3.42E-01	±	5.57E-03
^{206}Pb	(n,n)	^{206}Pb	(n,n')	3.30E-01	±	2.45E-02
^{208}Pb	(n,n')	^{208}Pb	(n,n')	3.19E-01	±	2.19E-02
^{240}Pu	(n,γ)	^{240}Pu	(n,γ)	3.17E-01	±	3.50E-03
			ρ total uncertainty (%) =	2.18E+00	±	9.86E-02

Table 23. ISC for the major contributions to the ρ_{VOID} uncertainty in Void Scenario 3 due to nuclear data. ISC obtained with MCNP(JEFF-3.3.)+SUMMON.

	Quantity		ρISC		
Void height = 18 cm	^{239}Pu	Total Fission ν	-9.174E-01	±	3.192E-02
	^{239}Pu	Prompt Fission ν	-9.151E-01	±	3.179E-02
	^{239}Pu	Fission	-7.746E-01	±	3.269E-02
	^{16}O	Elastic	2.239E-01	±	1.041E-01
	^{238}U	(n,γ)	1.945E-01	±	4.480E-03
	^{241}Pu	Total Fission ν	-1.656E-01	±	5.347E-03
	^{241}Pu	Prompt Fission ν	-1.646E-01	±	5.316E-03
	^{238}U	Inelastic	-1.435E-01	±	3.370E-02
	^{238}U	Total Fission ν	1.430E-01	±	7.419E-03
	^{238}U	Prompt Fission ν	1.412E-01	±	7.313E-03
Void height = 34 cm	^{239}Pu	Total Fission ν	-9.314E-01	±	2.002E-02
	^{239}Pu	Prompt Fission ν	-9.291E-01	±	1.995E-02
	^{239}Pu	Fission	-7.823E-01	±	2.036E-02
	^{238}U	(n,γ)	2.007E-01	±	2.830E-03
	^{209}Bi	Elastic	-1.768E-01	±	7.990E-02
	^{241}Pu	Total Fission ν	-1.683E-01	±	3.342E-03
	^{241}Pu	Prompt Fission ν	-1.673E-01	±	3.324E-03
	^{238}U	Total Fission ν	1.577E-01	±	4.781E-03
	^{238}U	Prompt Fission ν	1.559E-01	±	4.700E-03
	^{241}Pu	Fission	-1.363E-01	±	3.410E-03
Void height = 72 cm	^{239}Pu	Total Fission ν	-1.014E+00	±	1.776E-02
	^{239}Pu	Prompt Fission ν	-1.011E+00	±	1.768E-02
	^{239}Pu	Fission	-8.304E-01	±	1.805E-02
	^{209}Bi	Elastic	-3.260E-01	±	7.111E-02
	^{238}U	(n,γ)	2.514E-01	±	2.558E-03
	^{238}U	Total Fission ν	2.278E-01	±	4.367E-03
	^{238}U	Prompt Fission ν	2.250E-01	±	4.303E-03
	^{241}Pu	Total Fission ν	-1.846E-01	±	3.006E-03
	^{241}Pu	Prompt Fission ν	-1.836E-01	±	2.986E-03
	^{16}O	Elastic	1.800E-01	±	6.103E-02

To sum up, for smaller void volumes elastic and inelastic reactions have a relatively higher impact on the void worth value uncertainty. However, given the poor convergence of the sensitivity calculations with these reactions, it is very difficult to be conclusive about them. For larger void volumes, elastic and inelastic reactions still have a noticeable impact, in particular the calculations seem to be precise enough to identify ^{206}Pb (n,n′) and ^{238}U (n,n′) as the largest contributors to the uncertainty. Some fission reactions for uranium and plutonium isotopes also appear as significant contributors.

3.4. CONTROL RODS

The reactivity response due to the control rod insertion was calculated for two scenarios: in the first scenario, the buoyancy-driven control rods are fully inserted in the core while the gravity-safety control rods are fully out, in the second scenario both buoyancy-driven and gravity-safety control rods are fully inserted. As was expected the second scenario implies a higher reactivity response and a decrease of the criticality constant.

Table 24. Reactivity response due to control rods. The first column presents the criticality constant and reactivity worth value of a scenario with only the buoyancy-driven control rods fully inserted; the second column also incorporates the gravity-safety control rods fully inserted.

	MYRRHA - JEFF-3.3 - Control rods					
	BD			BD+GS		
k_{eff}	0.98824	±	0.00003	0.97461	±	0.00003
Δρ (pcms)	-2709	±	4	-4124	±	4

Table 25 lists the major contributors to the uncertainty in the first scenario with the buoyancy-driven control rods fully inserted. Here ^{240}Pu fissions are the main contributors to the uncertainty (1.21% being 2.10% the total contribution due to nuclear data), as it was the case of k_{eff}, although the highest sensitivity was to ^{239}Pu fissions. These results are very similar in the second scenario when safety control rods are also fully inserted as it can be seen in Table 26 (also 1.21% related to ^{240}Pu fissions being 1.87% the total contribution due to nuclear data).

Table 25. Reactions with the largest contributions to the uncertainty in the reactivity worth value of the MYRRHA homogenized model when buoyancy-driven control rods are fully in but gravity-safety rods are fully out. Scenario calculated with MCNP+KSEN2sdf+SUMMON with JEFF-3.3 library.

MYRRHA - JEFF-3.3 – Buoyancy-driven control rods fully in						
Quantity				ρ uncertainty (%)		
^{240}Pu	(n,f)	^{240}Pu	(n,f)	1.21E+00	±	3.51E-02
^{239}Pu	Total Fission χ	^{239}Pu	Total Fission χ	7.62E-01	±	1.50E-01
^{56}Fe	(n,n)	^{56}Fe	(n,n)	6.46E-01	±	1.61E-01
^{238}U	(n,n')	^{238}U	(n,n')	5.60E-01	±	1.90E-02
^{239}Pu	(n,f)	^{239}Pu	(n,f)	-5.29E-01	±	2.65E-02
^{238}U	(n,n')	^{238}U	(n,f)	5.19E-01	±	1.64E-02
^{240}Pu	(n,f)	^{240}Pu	(n,γ)	4.72E-01	±	1.24E-02
^{239}Pu	(n,γ)	^{239}Pu	(n,γ)	4.54E-01	±	1.92E-01
^{238}U	(n,n')	^{238}U	(n,γ)	-4.01E-01	±	1.06E-02
^{240}Pu	(n,n')	^{240}Pu	(n,f)	-3.89E-01	±	1.14E-02
^{239}Pu	(n,f)	^{239}Pu	(n,γ)	-3.29E-01	±	5.93E-03
^{238}U	(n,n)	^{238}U	(n,n')	-3.26E-01	±	7.56E-02
^{238}U	(n,f)	^{238}U	(n,f)	3.21E-01	±	1.57E-02
^{241}Pu	(n,n)	^{241}Pu	(n,n)	3.04E-01	±	1.85E-01
^{208}Pb	(n,n)	^{208}Pb	(n,n)	2.96E-01	±	1.75E-01
^{238}U	(n,γ)	^{238}U	(n,γ)	2.71E-01	±	4.80E-03
^{57}Fe	(n,n)	^{57}Fe	(n,n)	2.57E-01	±	1.10E-02
^{239}Pu	Prompt Fission ν	^{239}Pu	Prompt Fission ν	2.53E-01	±	6.01E-02
^{241}Pu	Total Fission χ	^{241}Pu	Total Fission χ	2.40E-01	±	1.15E-01
^{238}U	(n,n)	^{238}U	(n,f)	2.35E-01	±	1.16E-02
			ρ total uncertainty (%) =	1.96E+00	±	9.99E-02

Table 26. Reactions with the largest contributions to the uncertainty in the reactivity difference of the MYRRHA homogenized model when gravity-safety and buoyancy-driven control rods are fully in. Scenario calculated with MCNP+KSEN2sdf+SUMMON with JEFF-3.3 library.

MYRRHA - JEFF-3.3 – Buoyancy-driven and gravity-safety control rods fully in						
Quantity				ρ uncertainty (%)		
^{240}Pu	(n,f)	^{240}Pu	(n,f)	1.21E+00	±	2.24E-02
^{239}Pu	Total Fission χ	^{239}Pu	Total Fission χ	7.12E-01	±	9.95E-02
^{238}U	(n,n')	^{238}U	(n,n')	6.67E-01	±	1.18E-01
^{239}Pu	(n,f)	^{239}Pu	(n,f)	5.62E-01	±	1.21E-02
^{238}U	(n,n')	^{238}U	(n,f)	-5.24E-01	±	1.76E-02
^{240}Pu	(n,f)	^{240}Pu	(n,γ)	4.98E-01	±	1.10E-02
^{238}U	(n,n')	^{238}U	(n,γ)	-4.18E-01	±	7.84E-03
^{239}Pu	(n,γ)	^{239}Pu	(n,γ)	4.16E-01	±	8.00E-03
^{56}Fe	(n,n)	^{56}Fe	(n,n)	3.95E-01	±	1.36E-01
^{238}U	(n,n)	^{238}U	(n,n')	-3.81E-01	±	6.47E-02
^{238}U	(n,f)	^{238}U	(n,f)	3.19E-01	±	1.05E-02
^{239}Pu	(n,f)	^{239}Pu	(n,γ)	-3.18E-01	±	4.17E-03
^{238}U	(n,n)	^{238}U	(n,f)	2.75E-01	±	9.11E-03
^{239}Pu	Prompt Fission ν	^{239}Pu	Prompt Fission ν	2.56E-01	±	6.90E-03
^{238}U	(n,γ)	^{238}U	(n,γ)	2.47E-01	±	3.37E-03
^{10}B	(n,α)	^{10}B	(n,α)	2.13E-01	±	4.72E-04
^{241}Pu	Total Fission χ	^{241}Pu	Total Fission χ	2.10E-01	±	3.89E-02
^{16}O	(n,n)	^{16}O	(n,n)	1.91E-01	±	9.78E-02
^{240}Pu	(n,n')	^{240}Pu	(n,f)	-1.88E-01	±	4.12E-03
^{57}Fe	(n,n)	^{57}Fe	(n,n)	1.82E-01	±	5.40E-02
			ρ total uncertainty (%) =	1.85E+00	±	6.12E-02

Table 27. ISC for the major contributions to the ρ uncertainty when the control rods are fully inserted due to nuclear data. ISC obtained with MCNP(JEFF-3.3.)+SUMMON.

	Quantity		β_{eff}ISC		
Buoyancy-driven control rods fully in	^{239}Pu	Fission	7.175E-01	±	2.395E-02
	^{10}B	(n,α)	-6.481E-01	±	1.990E-03
	^{239}Pu	Total Fission ν	5.788E-01	±	2.381E-02
	^{239}Pu	Prompt Fission ν	5.782E-01	±	2.373E-02
	^{238}U	(n,γ)	1.683E-01	±	3.119E-03
	^{238}U	Total Fission ν	1.566E-01	±	5.341E-03
	^{208}Pb	Elastic	1.553E-01	±	6.427E-02
	^{238}U	Prompt Fission ν	1.546E-01	±	5.158E-03
	^{240}Pu	Total Fission ν	1.541E-01	±	3.792E-03
	^{240}Pu	Prompt Fission ν	1.538E-01	±	3.782E-03
Buoyancy-driven and gravity-safety	^{239}Pu	Fission	7.021E-01	±	1.500E-02
	^{10}B	(n,α)	-6.337E-01	±	1.399E-03
	^{239}Pu	Total Fission ν	5.775E-01	±	1.490E-02
	^{239}Pu	Prompt Fission ν	5.769E-01	±	1.484E-02
	^{238}U	Total Fission ν	1.564E-01	±	3.370E-03
	^{238}U	Prompt Fission ν	1.545E-01	±	3.324E-03
	^{238}U	(n,γ)	1.532E-01	±	2.179E-03
	^{240}Pu	Total Fission ν	1.528E-01	±	2.592E-03
	^{240}Pu	Prompt Fission ν	1.525E-01	±	2.585E-03
	^{240}Pu	Fission	1.353E-01	±	2.552E-03

The buoyancy-driven and gravity-safety control rods fully inserted is another case selected for determining the error in the total uncertainty from the standard deviation of a number (eight) of Monte Carlo calculations with different random number sequences:

$$\rho_{VOID} \text{ total uncertainty (\%)} = 1.75 \pm 0.05$$

This result is fully compatible with the total uncertainty listed in Table 26.

Also, some of the reactions with high contribution to the uncertainty were analysed by this methodology:

[^{240}Pu(n,f) - ^{240}Pu(n,f)] uncertainty contribution (%) = 1.20 ± 0.01
[^{239}Pu(Total Fission χ) -^{239}Pu(Total Fission χ)] uncertainty contribution (%) = 0.70 ± 0.08
[^{238}U(n,n) – ^{238}U(n,n)] uncertainty contribution (%) = 0.51 ± 0.06

In this case, the errors obtained in this way are comparable with those listed in Table 26.

3.5. DOPPLER COEFFICIENT

In this report, the Doppler effect was studied for the 8 different temperatures listed in Table 28. These temperature changes only affect the fuel materials. As it can be seen in Figure 7 the effect of the temperature on the criticality constant is essentially logarithmic.

Table 28. Criticality constant vs temperature.

T (K)	k_{eff}
600	1.01660 ± 0.00003
900	1.01485 ± 0.00003
1200	1.01375 ± 0.00003
1500	1.01289 ± 0.00003
1800	1.01210 ± 0.00003
2100	1.01159 ± 0.00003
2400	1.01104 ± 0.00003
3000	1.01024 ± 0.00003

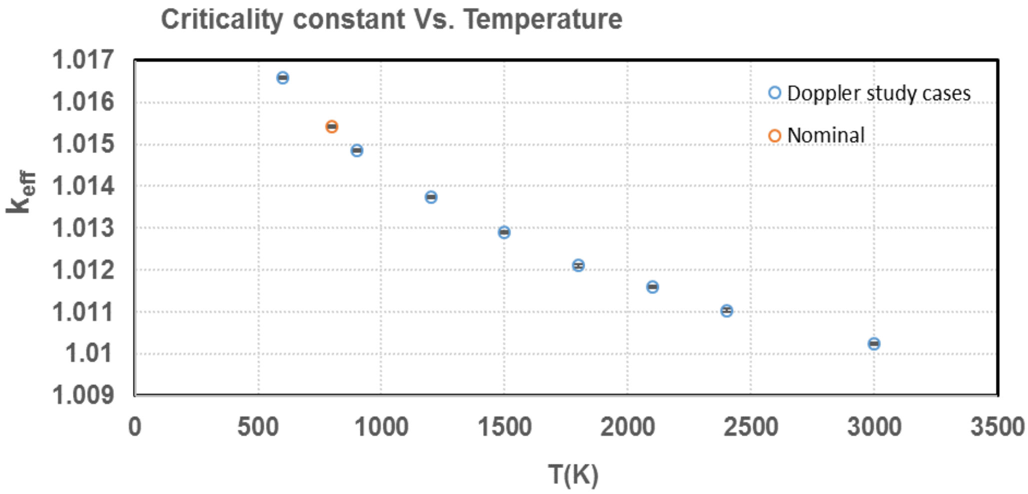

Figure 7. Criticality constant behaviour with the temperature.

The Doppler coefficient was calculated as the reactivity worth value divided by the temperature difference with the nominal case:

$$\rho_T = \frac{\Delta\rho}{T_{pert} - T_{nom}} \quad (3.5.1)$$

As it can be seen in Figure 8 the effect on the reactivity is also, as expected, essentially logarithmic with respect to the temperature increase. The large uncertainties observed in some points of Figure 8 are due to the small difference between the perturbed and nominal case temperatures.

In Table 29 ISC for the major contributors to the uncertainty of the Doppler coefficient is listed for these 8 temperatures. Elastic reactions of structural and coolant materials have a higher impact on the uncertainty, especially in lower temperature differences. As temperature difference (and hence calculation precission) increases (n,f), ν_{Total} and ν_{Prompt} of isotopes ^{239}Pu, ^{240}Pu and ^{238}U become dominant.

In Table 30 to Table 37, reactions with the largest contribution to the uncertainty are listed for the eight requested temperatures. For lower temperature cases, the main contributors are the elastic and inelastic reactions in elements of the structural materials, coolant and fuel such as O, Mg, Mn, Fe, Ni, Pb, U and Pu. With the temperature increase in the fuel materials, fission reactions also gain importance in the contribution to the uncertainty, although scattering reactions remain dominant. The large statistical uncertainty, however, does not allow to be conclusive about it.

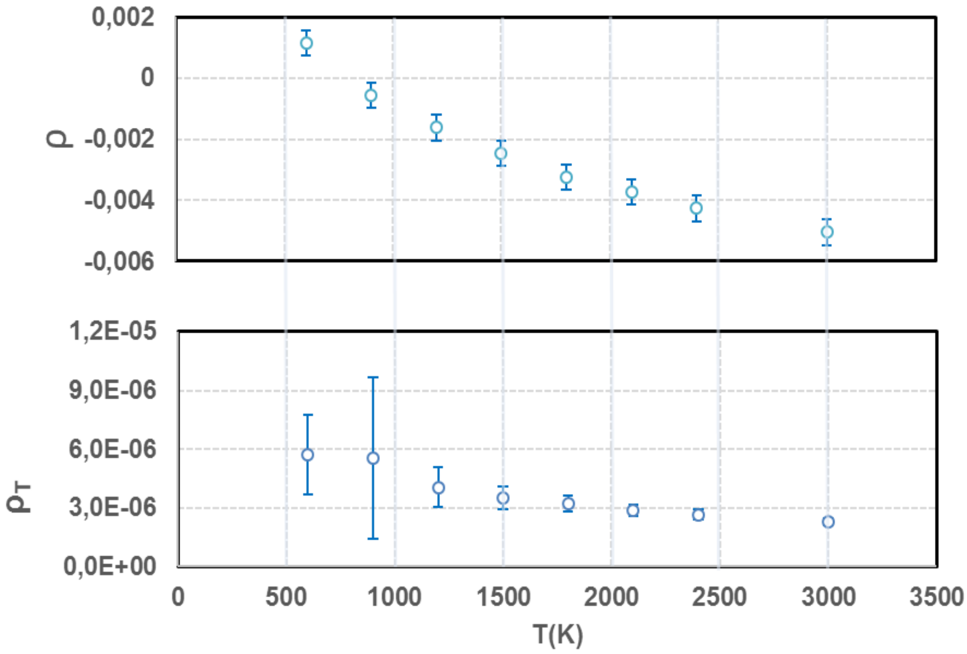

Figure 8. Reactivity and Doppler Coefficient.

Table 29. ISC for the major contributions to the ρ uncertainty due to nuclear data. ISC obtained with MCNP(JEFF-3.3.)+SUMMON.

T (K)	Quantity		ρISC		
600 K	^{16}O	Elastic	3.628E+00	±	1.777E+00
	^{56}Fe	Elastic	2.137E+00	±	1.808E+00
	^{209}Bi	Elastic	1.385E+00	±	2.272E+00
	^{208}Pb	Elastic	1.229E+00	±	1.605E+00
	^{239}Pu	Fission	-1.014E+00	±	5.404E-01
	^{56}Fe	Inelastic	-8.786E-01	±	3.048E-01
	^{206}Pb	Elastic	7.915E-01	±	9.603E-01
	^{239}Pu	Elastic	7.647E-01	±	7.765E-01
	^{239}Pu	Prompt Fission ν	-6.252E-01	±	5.277E-01
	^{239}Pu	Total Fission ν	-6.251E-01	±	5.298E-01

900K	^{16}O	Elastic	1.107E+01	±	3.648E+00
	^{238}U	Elastic	-3.554E+00	±	3.396E+00
	^{58}Ni	Elastic	-3.551E+00	±	1.709E+00
	^{207}Pb	Elastic	2.962E+00	±	2.139E+00
	^{240}Pu	Elastic	-1.896E+00	±	1.168E+00
	^{1}H	Elastic	1.617E+00	±	6.284E-01
	^{239}Pu	Fission	1.389E+00	±	1.136E+00
	^{27}Al	Elastic	-1.338E+00	±	8.741E-01
	^{209}Bi	Elastic	1.293E+00	±	4.943E+00
	^{56}Fe	Elastic	-1.107E+00	±	4.071E+00
1200 K	^{16}O	Elastic	1.449E+00	±	1.236E+00
	^{239}Pu	Fission	1.067E+00	±	3.836E-01
	^{58}Ni	Elastic	-1.004E+00	±	6.111E-01
	^{206}Pb	Elastic	8.876E-01	±	6.871E-01
	^{56}Fe	Elastic	5.725E-01	±	1.265E+00
	^{53}Cr	Elastic	5.508E-01	±	3.327E-01
	^{239}Pu	Total Fission ν	5.494E-01	±	3.775E-01
	^{239}Pu	Prompt Fission ν	5.491E-01	±	3.760E-01
	^{0}C	Elastic	4.713E-01	±	2.485E-01
	^{56}Fe	Inelastic	-4.346E-01	±	2.120E-01

1500 K	^{239}Pu	Fission	1.137E+00	±	2.619E-01
	^{56}Fe	Elastic	6.379E-01	±	8.450E-01
	^{239}Pu	Prompt Fission ν	5.761E-01	±	2.549E-01
	^{239}Pu	Total Fission ν	5.757E-01	±	2.559E-01
	^{209}Bi	Elastic	-5.460E-01	±	1.137E+00
	^{58}Ni	Elastic	-5.355E-01	±	3.999E-01
	^{240}Pu	Elastic	-4.368E-01	±	2.476E-01
	^{206}Pb	Elastic	4.319E-01	±	4.563E-01
	^{207}Pb	Elastic	3.975E-01	±	4.484E-01
	^{16}O	Elastic	3.791E-01	±	8.282E-01

1800 K	^{209}Bi	Elastic	1.246E+00	±	8.554E-01
	^{239}Pu	Fission	1.137E+00	±	1.892E-01
	^{239}Pu	Total Fission ν	6.342E-01	±	1.876E-01
	^{239}Pu	Prompt Fission ν	6.334E-01	±	1.869E-01
	^{208}Pb	Elastic	5.934E-01	±	5.689E-01
	^{52}Cr	Elastic	3.613E-01	±	2.680E-01
	^{239}Pu	(n,γ)	3.134E-01	±	1.950E-02
	^{207}Pb	Elastic	2.843E-01	±	3.535E-01

	^{240}Pu	Elastic	-2.669E-01	±	1.962E-01
	^{238}U	Inelastic	-2.451E-01	±	2.020E-01

2100 K	^{239}Pu	Fission	1.079E+00	±	1.719E-01
	^{16}O	Elastic	9.443E-01	±	5.698E-01
	^{208}Pb	Elastic	6.220E-01	±	4.837E-01
	^{239}Pu	Total Fission ν	6.034E-01	±	1.704E-01
	^{239}Pu	Prompt Fission ν	6.023E-01	±	1.696E-01
	^{56}Fe	Elastic	4.323E-01	±	5.587E-01
	^{58}Ni	Elastic	-4.065E-01	±	2.544E-01
	^{238}U	Elastic	3.587E-01	±	4.892E-01
	^{54}Fe	Elastic	-3.301E-01	±	1.971E-01
	^{238}U	Inelastic	-3.195E-01	±	1.671E-01

2400 K	^{239}Pu	Fission	1.134E+00	±	1.449E-01
	^{209}Bi	Elastic	9.460E-01	±	6.293E-01
	^{239}Pu	Total Fission ν	6.082E-01	±	1.428E-01
	^{239}Pu	Prompt Fission ν	6.079E-01	±	1.423E-01
	^{16}O	Elastic	5.977E-01	±	4.662E-01
	^{207}Pb	Elastic	5.288E-01	±	2.596E-01
	^{238}U	Elastic	4.783E-01	±	4.544E-01
	^{239}Pu	(n,γ)	3.158E-01	±	1.374E-02
	^{238}U	Inelastic	-3.155E-01	±	1.346E-01
	^{240}Pu	Elastic	-2.453E-01	±	1.440E-01

3000 K	^{239}Pu	Fission	1.154E+00	±	1.264E-01
	^{209}Bi	Elastic	6.632E-01	±	5.177E-01
	^{239}Pu	Total Fission ν	6.376E-01	±	1.249E-01
	^{239}Pu	Prompt Fission ν	6.371E-01	±	1.245E-01
	^{56}Fe	Elastic	6.136E-01	±	4.241E-01
	^{238}U	Elastic	4.158E-01	±	3.787E-01
	^{239}Pu	(n,γ)	3.223E-01	±	1.203E-02
	^{238}U	Inelastic	-3.149E-01	±	1.244E-01
	^{207}Pb	Elastic	2.981E-01	±	2.313E-01
	^{58}Ni	Elastic	-2.650E-01	±	1.979E-01

Table 30. Doppler case T = 600 K. Reactions with the largest contributions to the uncertainty in the reactivity of the MYRRHA homogenized model. Scenario calculated with MCNP+KSEN2sdf+SUMMON with JEFF-3.3 library.

MYRRHA - JEFF-3.3 – Doppler (T = 600 K)						
Quantity				ρ uncertainty (%)		
^{57}Fe	(n,n)	^{57}Fe	(n,n)	7.84E+00	±	3.27E+00
^{16}O	(n,n)	^{16}O	(n,n)	7.16E+00	±	3.49E+00
^{56}Fe	(n,n)	^{56}Fe	(n,n)	6.70E+00	±	3.36E+00
^{58}Ni	(n,n)	^{58}Ni	(n,n)	4.59E+00	±	1.54E+00
^{54}Fe	(n,n)	^{54}Fe	(n,n)	4.16E+00	±	1.55E+00
^{60}Ni	(n,n)	^{60}Ni	(n,n)	4.07E+00	±	2.03E+00
^{238}U	(n,n)	^{238}U	(n,n)	3.91E+00	±	3.44E+00
^{58}Fe	(n,n)	^{58}Fe	(n,n)	3.12E+00	±	1.11E+00
^{208}Pb	(n,n)	^{208}Pb	(n,n)	3.09E+00	±	3.09E+00
^{241}Pu	(n,n')	^{241}Pu	(n,n')	3.08E+00	±	1.37E+00
^{240}Pu	(n,n')	^{240}Pu	(n,n')	2.93E+00	±	2.34E+00
^{240}Pu	(n,n)	^{240}Pu	(n,n')	-2.90E+00	±	2.23E+00
^{56}Fe	(n,n')	^{56}Fe	(n,n')	2.85E+00	±	8.01E-01
^{206}Pb	(n,n)	^{206}Pb	(n,n)	2.57E+00	±	9.84E-01
^{238}U	(n,n)	^{238}U	(n,n')	2.43E+00	±	1.10E+01
^{62}Ni	(n,n)	^{62}Ni	(n,n)	2.39E+00	±	1.63E+00
^{207}Pb	(n,n)	^{207}Pb	(n,n)	2.09E+00	±	7.76E-01
^{206}Pb	(n,n')	^{206}Pb	(n,n')	2.02E+00	±	1.51E+00
^{238}U	(n,n')	^{238}U	(n,n')	1.94E+00	±	3.40E+00
^{240}Pu	(n,f)	^{240}Pu	(n,f)	1.85E+00	±	8.12E-01
ρ total uncertainty (%) =				1.83E+01	±	3.22E+00

Table 31. Doppler case T = 900 K. Reactions with the largest contributions to the uncertainty in the reactivity of the MYRRHA homogenized model. Scenario calculated with MCNP+KSEN2sdf+SUMMON with JEFF-3.3 library.

MYRRHA - JEFF-3.3 – Doppler (T = 900 K)						
Quantity				ρ uncertainty (%)		
^{16}O	(n,n)	^{16}O	(n,n)	2.20E+01	±	7.17E+00
^{57}Fe	(n,n)	^{57}Fe	(n,n)	2.20E+01	±	6.90E+00
^{56}Fe	(n,n)	^{56}Fe	(n,n)	1.89E+01	±	1.21E+01
^{58}Ni	(n,n)	^{58}Ni	(n,n)	1.18E+01	±	4.84E+00
^{241}Pu	(n,n)	^{241}Pu	(n,n)	1.06E+01	±	8.90E+00
^{54}Fe	(n,n)	^{54}Fe	(n,n)	1.05E+01	±	3.49E+00
^{239}Pu	Total Fission χ	^{239}Pu	Total Fission χ	6.20E+00	±	7.12E+00
^{58}Fe	(n,n)	^{58}Fe	(n,n)	6.01E+00	±	2.09E+00
^{62}Ni	(n,n)	^{62}Ni	(n,n)	5.82E+00	±	3.73E+00
^{207}Pb	(n,n)	^{207}Pb	(n,n)	5.64E+00	±	2.64E+00
^{240}Pu	(n,n)	^{240}Pu	(n,n)	4.91E+00	±	3.81E+00
^{208}Pb	(n,n)	^{208}Pb	(n,n)	4.81E+00	±	3.62E+00
^{206}Pb	(n,n')	^{206}Pb	(n,n')	4.63E+00	±	4.51E+00
^{238}U	(n,n')	^{238}U	(n,n')	4.32E+00	±	5.17E+00
^{60}Ni	(n,n)	^{60}Ni	(n,n)	4.10E+00	±	3.68E+00
^{238}U	(n,n)	^{238}U	(n,n')	4.07E+00	±	1.15E+01
^{240}Pu	(n,n)	^{240}Pu	(n,n')	3.97E+00	±	1.15E+01
^{25}Mg	(n,n)	^{25}Mg	(n,n)	3.50E+00	±	1.72E+00
^{55}Mn	(n,n)	^{55}Mn	(n,n)	3.29E+00	±	4.29E+00
^{238}U	(n,n)	^{238}U	(n,n)	3.17E+00	±	7.06E+00
			ρ total uncertainty (%) =	4.59E+01	±	7.75E+00

Table 32. Doppler case T = 1200 K. Reactions with the largest contributions to the uncertainty in the reactivity of the MYRRHA homogenized model. Scenario calculated with MCNP+KSEN2sdf+SUMMON with JEFF-3.3 library.

MYRRHA - JEFF-3.3 – Doppler (T = 1200 K)						
Quantity				ρ uncertainty (%)		
^{58}Ni	(n,n)	^{58}Ni	(n,n)	5.68E+00	±	1.86E+00
^{57}Fe	(n,n)	^{57}Fe	(n,n)	5.57E+00	±	2.08E+00
^{56}Fe	(n,n)	^{56}Fe	(n,n)	4.57E+00	±	2.64E+00
^{208}Pb	(n,n)	^{208}Pb	(n,n)	4.09E+00	±	1.53E+00
^{16}O	(n,n)	^{16}O	(n,n)	2.68E+00	±	2.42E+00
^{241}Pu	(n,n)	^{241}Pu	(n,n)	2.42E+00	±	2.92E+00
^{238}U	(n,n)	^{238}U	(n,n)	2.40E+00	±	2.56E+00
^{206}Pb	(n,n')	^{206}Pb	(n,n')	1.90E+00	±	1.52E+00
^{238}U	(n,n)	^{238}U	(n,f)	1.88E+00	±	5.67E-01
^{62}Ni	(n,n)	^{62}Ni	(n,n)	1.80E+00	±	1.18E+00
^{54}Fe	(n,n)	^{54}Fe	(n,n)	1.75E+00	±	7.20E-01
^{27}Al	(n,n)	^{27}Al	(n,n)	1.64E+00	±	1.03E+00
^{206}Pb	(n,n)	^{206}Pb	(n,n')	1.59E+00	±	1.39E+00
^{238}U	Total Fission χ	^{238}U	Total Fission χ	1.58E+00	±	5.57E-01
^{207}Pb	(n,n')	^{207}Pb	(n,n')	1.49E+00	±	1.05E+00
^{55}Mn	(n,n)	^{55}Mn	(n,n)	1.46E+00	±	1.24E+00
^{56}Fe	(n,n')	^{56}Fe	(n,n')	1.39E+00	±	6.19E-01
^{206}Pb	(n,n)	^{206}Pb	(n,n)	1.38E+00	±	8.32E-01
^{240}Pu	(n,n')	^{240}Pu	(n,f)	-1.36E+00	±	7.76E-01
^{239}Pu	(n,γ)	^{239}Pu	(n,γ)	1.30E+00	±	2.15E-01
			ρ total uncertainty (%) =	1.32E+01	±	2.06E+00

Table 33. Doppler case T = 1500 K. Reactions with the largest contributions to the uncertainty in the reactivity of the MYRRHA homogenized model. Scenario calculated with MCNP+KSEN2sdf+SUMMON with JEFF-3.3 library.

MYRRHA - JEFF-3.3 – Doppler (T = 1500 K)						
Quantity				ρ uncertainty (%)		
^{56}Fe	(n,n)	^{56}Fe	(n,n)	4.69E+00	±	2.29E+00
^{57}Fe	(n,n)	^{57}Fe	(n,n)	4.21E+00	±	1.58E+00
^{239}Pu	Total Fission χ	^{239}Pu	Total Fission χ	3.52E+00	±	1.50E+00
^{238}U	(n,n')	^{238}U	(n,n')	2.53E+00	±	1.97E+00
^{58}Ni	(n,n)	^{58}Ni	(n,n)	2.36E+00	±	9.94E-01
^{62}Ni	(n,n)	^{62}Ni	(n,n)	1.44E+00	±	7.53E-01
^{240}Pu	(n,f)	^{240}Pu	(n,f)	1.37E+00	±	3.88E-01
^{240}Pu	(n,n)	^{240}Pu	(n,n)	1.37E+00	±	8.06E-01
^{238}U	(n,n)	^{238}U	(n,n')	1.30E+00	±	1.02E+00
^{239}Pu	(n,γ)	^{239}Pu	(n,γ)	1.22E+00	±	1.39E-01
^{239}Pu	(n,f)	^{239}Pu	(n,f)	1.19E+00	±	2.06E-01
^{238}U	(n,n')	^{238}U	(n,f)	-1.19E+00	±	4.18E-01
^{209}Bi	(n,n')	^{209}Bi	(n,n')	1.18E+00	±	4.59E-01
^{208}Pb	(n,n)	^{208}Pb	(n,n)	1.14E+00	±	1.35E+00
^{207}Pb	(n,n)	^{207}Pb	(n,n)	1.13E+00	±	3.60E-01
^{241}Pu	(n,n)	^{241}Pu	(n,n)	1.13E+00	±	2.00E+00
^{241}Pu	Total Fission χ	^{241}Pu	Total Fission χ	1.06E+00	±	6.15E-01
^{54}Fe	(n,n)	^{54}Fe	(n,n)	1.05E+00	±	4.66E-01
^{25}Mg	(n,n)	^{25}Mg	(n,n)	1.02E+00	±	3.74E-01
^{58}Fe	(n,n)	^{58}Fe	(n,n)	1.02E+00	±	4.61E-01
ρ total uncertainty (%) =				9.59E+00	±	1.67E+00

Table 34. Doppler case T = 1800 K. Reactions with the largest contributions to the uncertainty in the reactivity of the MYRRHA homogenized model. Scenario calculated with MCNP+KSEN2sdf+SUMMON with JEFF-3.3 library.

MYRRHA - JEFF-3.3 – Doppler (T = 1800 K)						
Quantity				ρ uncertainty (%)		
^{56}Fe	(n,n)	^{56}Fe	(n,n)	3.57E+00	±	2.10E+00
^{239}Pu	Total Fission χ	^{239}Pu	Total Fission χ	2.71E+00	±	1.18E+00
^{57}Fe	(n,n)	^{57}Fe	(n,n)	2.43E+00	±	9.45E-01
^{208}Pb	(n,n)	^{208}Pb	(n,n)	2.23E+00	±	1.42E+00
^{54}Fe	(n,n)	^{54}Fe	(n,n)	2.05E+00	±	7.71E-01
^{238}U	(n,n')	^{238}U	(n,n')	1.90E+00	±	1.48E+00
^{58}Ni	(n,n)	^{58}Ni	(n,n)	1.52E+00	±	7.40E-01
^{240}Pu	(n,f)	^{240}Pu	(n,f)	1.34E+00	±	2.70E-01
^{240}Pu	(n,n)	^{240}Pu	(n,n)	1.27E+00	±	6.36E-01
^{239}Pu	(n,γ)	^{239}Pu	(n,γ)	1.24E+00	±	1.06E-01
^{10}B	(n,n')	^{10}B	(n,n')	1.15E+00	±	1.10E+00
^{239}Pu	(n,f)	^{239}Pu	(n,f)	1.12E+00	±	1.50E-01
^{240}Pu	(n,n)	^{240}Pu	(n,n')	9.47E-01	±	2.09E+00
^{240}Pu	(n,f)	^{240}Pu	(n,γ)	8.89E-01	±	8.55E-02
^{238}U	(n,n')	^{238}U	(n,f)	-8.72E-01	±	3.27E-01
^{241}Pu	Total Fission χ	^{241}Pu	Total Fission χ	8.29E-01	±	4.79E-01
^{239}Pu	(n,f)	^{239}Pu	(n,γ)	-8.00E-01	±	3.90E-02
^{241}Pu	(n,n')	^{241}Pu	(n,n')	7.47E-01	±	4.36E-01
^{240}Pu	(n,n')	^{240}Pu	(n,f)	-7.05E-01	±	1.35E-01
^{240}Pu	(n,n)	^{240}Pu	(n,f)	-6.99E-01	±	1.81E-01
			ρ total uncertainty (%) =	7.44E+00	±	1.36E+00

Table 35. Doppler case T = 2100 K. Reactions with the largest contributions to the uncertainty in the reactivity of the MYRRHA homogenized model. Scenario calculated with MCNP+KSEN2sdf+SUMMON with JEFF-3.3 library.

MYRRHA - JEFF-3.3 – Doppler (T = 2100 K)						
Quantity				ρ uncertainty (%)		
^{56}Fe	(n,n)	^{56}Fe	(n,n)	3.00E+00	±	1.57E+00
^{54}Fe	(n,n)	^{54}Fe	(n,n)	2.52E+00	±	9.84E-01
^{238}U	(n,n')	^{238}U	(n,n')	2.17E+00	±	1.17E+00
^{58}Ni	(n,n)	^{58}Ni	(n,n)	1.94E+00	±	7.32E-01
^{16}O	(n,n)	^{16}O	(n,n)	1.89E+00	±	1.12E+00
^{239}Pu	Total Fission χ	^{239}Pu	Total Fission χ	1.59E+00	±	1.01E+00
^{208}Pb	(n,n)	^{208}Pb	(n,n)	1.47E+00	±	9.33E-01
^{240}Pu	(n,f)	^{240}Pu	(n,f)	1.43E+00	±	2.39E-01
^{239}Pu	(n,γ)	^{239}Pu	(n,γ)	1.15E+00	±	9.03E-02
^{239}Pu	(n,f)	^{239}Pu	(n,f)	1.14E+00	±	1.40E-01
^{238}U	(n,n')	^{238}U	(n,f)	-1.12E+00	±	2.83E-01
^{57}Fe	(n,n)	^{57}Fe	(n,n)	1.09E+00	±	5.75E-01
^{238}U	(n,n)	^{238}U	(n,n')	-1.03E+00	±	4.77E-01
^{240}Pu	(n,n')	^{240}Pu	(n,f)	-8.71E-01	±	1.41E-01
^{240}Pu	(n,f)	^{240}Pu	(n,γ)	8.56E-01	±	8.77E-02
^{239}Pu	(n,f)	^{239}Pu	(n,γ)	-7.49E-01	±	3.71E-02
^{56}Fe	(n,γ)	^{56}Fe	(n,γ)	6.77E-01	±	6.28E-02
^{240}Pu	(n,n)	^{240}Pu	(n,n')	6.70E-01	±	8.90E-01
^{206}Pb	(n,n)	^{206}Pb	(n,n)	6.61E-01	±	2.91E-01
^{60}Ni	(n,n)	^{60}Ni	(n,n)	6.45E-01	±	5.87E-01
			ρ total uncertainty (%) =	6.55E+00	±	1.04E+00

Table 36. Doppler case T = 2400 K. Reactions with the largest contributions to the uncertainty in the reactivity of the MYRRHA homogenized model. Scenario calculated with MCNP+KSEN2sdf+SUMMON with JEFF-3.3 library.

MYRRHA - JEFF-3.3 – Doppler (T = 2400 K)						
Quantity				ρ uncertainty (%)		
^{238}U	(n,n)	^{238}U	(n,n')	-2.60E+00	±	1.10E+00
^{238}U	(n,n')	^{238}U	(n,n')	2.24E+00	±	9.74E-01
^{238}U	(n,n)	^{238}U	(n,n)	1.76E+00	±	9.64E-01
^{239}Pu	Total Fission χ	^{239}Pu	Total Fission χ	1.58E+00	±	9.47E-01
^{240}Pu	(n,f)	^{240}Pu	(n,f)	1.55E+00	±	2.13E-01
^{241}Pu	(n,n)	^{241}Pu	(n,n)	1.50E+00	±	1.19E+00
^{57}Fe	(n,n)	^{57}Fe	(n,n)	1.45E+00	±	6.99E-01
^{239}Pu	(n,γ)	^{239}Pu	(n,γ)	1.36E+00	±	7.76E-02
^{54}Fe	(n,n)	^{54}Fe	(n,n)	1.22E+00	±	4.07E-01
^{207}Pb	(n,n)	^{207}Pb	(n,n)	1.18E+00	±	3.56E-01
^{16}O	(n,n)	^{16}O	(n,n)	1.16E+00	±	9.15E-01
^{240}Pu	(n,n)	^{240}Pu	(n,n')	-1.14E+00	±	7.95E-01
^{238}U	(n,n)	^{238}U	(n,f)	1.13E+00	±	2.69E-01
^{240}Pu	(n,n')	^{240}Pu	(n,f)	1.06E+00	±	1.48E-01
^{238}U	(n,n')	^{238}U	(n,f)	-1.04E+00	±	2.55E-01
^{208}Pb	(n,n)	^{208}Pb	(n,n)	1.01E+00	±	7.01E-01
^{239}Pu	(n,f)	^{239}Pu	(n,f)	9.70E-01	±	1.14E-01
^{56}Fe	(n,n)	^{56}Fe	(n,n)	9.58E-01	±	9.97E-01
^{58}Ni	(n,n)	^{58}Ni	(n,n)	9.49E-01	±	5.82E-01
^{240}Pu	(n,f)	^{240}Pu	(n,γ)	8.92E-01	±	7.44E-02
			ρ total uncertainty (%) =	5.41E+00	±	7.11E-01

Table 37. Doppler case T = 3000 K. Reactions with the largest contributions to the uncertainty in the reactivity of the MYRRHA homogenized model. Scenario calculated with MCNP+KSEN2sdf+SUMMON with JEFF-3.3 library.

MYRRHA - JEFF-3.3 – Doppler (T = 3000 K)						
Quantity				ρ uncertainty (%)		
^{238}U	(n,n')	^{238}U	(n,n')	2.10E+00	±	8.46E-01
^{56}Fe	(n,n)	^{56}Fe	(n,n)	1.97E+00	±	1.23E+00
^{57}Fe	(n,n)	^{57}Fe	(n,n)	1.90E+00	±	6.39E-01
^{238}U	(n,n)	^{238}U	(n,n')	-1.75E+00	±	6.96E-01
^{239}Pu	(n,γ)	^{239}Pu	(n,γ)	1.37E+00	±	6.52E-02
^{240}Pu	(n,f)	^{240}Pu	(n,f)	1.36E+00	±	1.83E-01
^{208}Pb	(n,n)	^{208}Pb	(n,n)	1.11E+00	±	8.48E-01
^{238}U	(n,n')	^{238}U	(n,f)	-1.04E+00	±	2.45E-01
^{58}Ni	(n,n)	^{58}Ni	(n,n)	1.03E+00	±	5.06E-01
^{239}Pu	(n,f)	^{239}Pu	(n,f)	9.90E-01	±	9.77E-02
^{54}Fe	(n,n)	^{54}Fe	(n,n)	9.05E-01	±	4.99E-01
^{240}Pu	(n,n)	^{240}Pu	(n,n')	8.74E-01	±	7.20E-01
^{238}U	(n,n)	^{238}U	(n,n)	8.46E-01	±	7.69E-01
^{240}Pu	(n,f)	^{240}Pu	(n,γ)	8.32E-01	±	6.04E-02
^{240}Pu	(n,n')	^{240}Pu	(n,f)	-8.26E-01	±	1.04E-01
^{238}U	(n,n)	^{238}U	(n,f)	7.73E-01	±	1.82E-01
^{239}Pu	(n,f)	^{239}Pu	(n,γ)	-7.28E-01	±	2.78E-02
^{58}Fe	(n,n)	^{58}Fe	(n,n)	7.07E-01	±	2.49E-01
^{240}Pu	(n,n)	^{240}Pu	(n,n)	6.86E-01	±	4.13E-01
^{239}Pu	Total Fission χ	^{239}Pu	Total Fission χ	6.74E-01	±	7.80E-01
			ρ total uncertainty (%) =	4.91E+00	±	6.86E-01

4. CONCLUSIONS

S/U analyses have been performed for the homogenized MYRRHA design version 1.8, using MCNP 6.2, SUMMON and the JEFF-3.3 library (with its covariance matrices processed in 33 groups of energy) for relevant reactor parameters, namely k_{eff}, β_{eff}, Doppler reactivity coefficients, void worth and reactivity worth of control rods.

The total uncertainty due to nuclear data has been found to be around 0.76 ± 0.01% for k_{eff} and around 6.82 ± 1.12 % and 1.26 ± 0.04 % for β_{eff} with Brescher and Chiba methodologies respectively. The statistical uncertainties of these figures have been compared with the results of some Monte Carlo calculations with different random number sequences. Largest contributors to the uncertainty in k_{eff} is ^{240}Pu (n,f) with other reactions of ^{240}Pu as well as ^{238}U and ^{239}Pu having also significant contributions. Concerning β_{eff}, since covariance data for the delayed neutron ν of most relevant isotopes is missing in the JEFF-3.3 libraries, the figures of the uncertainty due to nuclear data obtained in this study are likely to be underestimated.

Concerning the void reactivity effect, four scenarios (denoted as 0, 1, 2 and 3) have been considered with an increased number of voided elements. For each of these scenarios, three heights have been considered. In void scenario 0, the reactivity effect is small and the resulting statistical uncertainties are too large to be significant. In Void Scenario 1, the total uncertainty due to nuclear data in the void reactivity worth is between 11 and 31%, in Void Scenario 2 between 8 and 13%, and in Void Scenario 3, between 1.8 and 2.2%. In the largest void scenarios, where the statistical convergence is better, largest contributions to the uncertainty were ^{206}Pb(n,n′) and ^{238}U(n,n′). Even in this last case we cannot assure the convergence of scattering reactions.

For the case of control rod worth, uncertainty due to nuclear data is 1.96 ± 0.10 % when only the buoyancy-driven control rods are fully inserted and 1.85 ± 0.06 % when the security rods are also inserted. As in the case of the k_{eff}, largest contributor to the uncertainty was ^{240}Pu (n,f).

In the eight Doppler cases, the largest contribution (18.3%) can be found in T(K)=600, where elastic reactions have the main contributions. However, the statistical uncertainty affecting these reactions is rather high and is difficult to extract conclusions from these results. Also, the second and third more important contributions due to nuclear data (13.2% and 9.6%) are found in T(K)=1200K and 1500K where apart from the elastic reactions of the T(K)=600K case some fission reactions of Pu isotopes and ^{238}U start to have a noticeable impact.

5. ACKNOWLEDGEMENTS

This work has been supported by the SANDA project (grant agreement 847552) of the EU Horizon 2020 framework program. MCNP and SCALE have been obtained through RSICC and NEA Computer Programs Services, respectively.

6. REFERENCES

[Barale 2020] H. Barale. *Application of the SERPENT code to neutronic analyses of the MYRRHA core: a sensitivity and uncertainty approach*. Politecnico di Torino MSc Thesis (2020).

[Bretscher 1997] Bretscher, M. M. *Perturbation-independent methods for calculating research reactor kinetic parameters*. ANL/RERTR/TM-30, Argonne National Laboratory (1997).

[Chiba 2009] Chiba, G., *Calculation of Effective Delayed Neutron Fraction Using a Modified k-Ratio Method*. J. Nucl. Sci. Technol. 46, 399–402.

[Fiorito 2019] L. Fiorito. *Neutronic design of the MYRRHA core version 1.8*. 5th International Workshop on Accelerator Driven Sub-Critical Systems & Thorium Utilisation. Mol (Belgium) 6-8 November 2019.

[Fiorito 2021a] L. Fiorito *et al*. *Homogenized neutronics model of MYRRHA design revision 1.8*. SCK CEN/44767116 (2021).

[Fiorito 2021b] L. Fiorito *et al*. *Requested neutronics parameters for SU analysis of MYRRHA Core*. SCK CEN/45347165 (2021).

[Hernandez-Solis, 2021] A. Hernandez-Solis. *Reactivity studies of the MYRRHA 1.6 core under void conditions*. SCK CEN/37834506 (2021).

[Iwamoto, 2018] Iwamoto, H., Stankovskiy, A., Fiorito, L., Van den Eynde, G., 2018. *Monte Carlo uncertainty quantification of the effective delayed neutron fraction*. J. Nucl. Sci. Technol. 55, 539-547.

[Kodeli 2015] I. Kodeli. *Effective delayed neutron fraction (βeff) sensitivity and uncertainty analysis of the MYRRHA reactor*. EC FP7 CHANDA Project Deliverable 10.1bis (2015).

[Malambu 2014] E. Malambu and A. Stankovskiy. *Revised Core Design for MYRRHA-Rev1.6*. SCK CEN/3958903 (2014).

[NJOY 21] NJOY21—NJOY for the 21st Century. https://www.njoy21.io. (accessed on 28 September 2022).

[Plompen 2020] A. J. M. Plompen et al., The joint evaluated fission and fusion nuclear data library, JEFF-3.3. European Physical Journal A 56 (2020) 181. DOI: 10.1140/epja/s10050-020-00141-9.

[Rearden 2018] B. T. Rearden and M. A. Jessee (Eds.). *SCALE Code System*. Oak Ridge National Laboratory report ORNL/TM-2005/39 Version 6.2.3 (2018).

[Romojaro 2015] P. Romojaro and F. Álvarez-Velarde. *Report on sensitivity analysis of MYRRHA with list of key reactions*. EC FP7 CHANDA Project Deliverable 10.1 (2015).

[Romojaro 2017] P. Romojaro *et al*., *SUMMON: A Sensitivity And Uncertainty Methodology For MONte Carlo Codes*. In M&C 2017 Conference, Jeju (Korea) 16-20 April 2017.

[Romojaro 2019] P. Romojaro. *Nuclear data analyses for improving the safety of advanced lead-cooled reactors*. Doctoral dissertation, Universidad Politécnica de Madrid (2019).

[SCK CEN 2021] https://www.sckcen.be/en/projects/myrrha (accessed on 26 Jan 2022).

[Werner 2017] Werner, C.J. (Ed.). *MCNP6 User's Manual, Code version 6.2*. Los Alamos National Laboratory Report LA-UR-17-29981.

FIRMANTE	NOMBRE	FECHA	NOTAS
FIRMANTE[1]	**SONIA PANIZO PRIETO**	**25/10/2022 13:37 | Sin acción específica**	
FIRMANTE[2]	**FRANCISCO ALVAREZ VELARDE**	**25/10/2022 14:52 | Sin acción específica**	
FIRMANTE[3]	**M.SOLEDAD FERNANDEZ FERNANDEZ**	**25/10/2022 15:02 | Sin acción específica**	
FIRMANTE[4]	**ENRIQUE MIGUEL GONZALEZ ROMERO**	**25/10/2022 15:33 | Sin acción específica**	